博士論文

Thrombopoietin/MPL signaling enhances growth and survival capacity of acute myeloid leukemia cells with high Evi1 expression

（トロンボポエチンシグナルは **Evi1** 高発現急性骨髄性白血病細胞の増殖および生存を促進する）

西川　慧

CONTENTS

Contents ····· **1**

Abstract ····· **2**

Introduction ····· **3**

Methods ····· **7**

Results ····· **21**

Discussion ····· **61**

Acknowledgments ····· **73**

References ····· **74**

Abstract

Ecotropic viral integration site 1 (Evi1) is a transcription factor that is highly expressed in hematopoietic stem cells and is crucial for their self-renewal capacity. Aberrant expression of EVI1 is observed in 5% to 10% of patients with de novo acute myeloid leukemia (AML) and predicts poor prognosis, reflecting the multiple leukemogenic properties of EVI1. Here, I show that thrombopoietin (THPO) signaling is implicated in the growth and survival of Evi1-expressing cells, using a mouse model of Evi1 leukemia. I first identified that the expression of megakaryocytic surface molecules such as *ITGA2B* (CD41) and the THPO receptor, *MPL*, positively correlates with *EVI1* expression in patients with AML. In agreement with this finding, a subpopulation of bone marrow and spleen cells derived from Evi1 leukemia mice expressed both CD41 and Mpl. $CD41^+$ Evi1 leukemia cells induced secondary leukemia more efficiently than $CD41^-$ cells in a serial bone marrow transplantation assay. Importantly, the $CD41^+$ cells predominantly expressing Mpl effectively proliferated and survived on OP9 stromal cells in the presence of THPO via upregulating BCL-xL expression, suggesting an essential role of the THPO/MPL/BCL-xL cascade in enhancing the progression of Evi1 leukemia. These observations provide a novel aspect of the diverse functions of Evi1 in leukemogenesis.

Introduction

Acute myeloid leukemia (AML) is a clonal hematological disorder in which somatically acquired genetic alterations in hematopoietic stem/progenitor cells (HSPCs) disturb their growth and differentiation. Chromosomal abnormalities or specific gene mutations are used in the risk classification of AML as prognostic biomarkers. In addition, distinct gene expression signatures have been utilized to identify the prognostic subclasses of AML.[1] Among these stratified groups, aberrant expression of ecotropic viral integration site 1 (EVI1) occurs in approximately 5% to 10% of de novo adult AML patients and defines one of the largest clusters in AML.[2-5] *EVI1* gene is located on chromosome 3q26 and its inappropriate expression is often caused by 3q abnormalities such as inv(3)(q21q26.2) or t(3;3)(q21;q26.2).[6] According to the World Health Organization classification, AML with inv(3)(q21q26.2) or t(3;3)(q21;q26.2) is associated with normal or elevated platelet counts and shows increased atypical bone marrow (BM) megakaryocytes and associated multilineage dysplasia.[7] Furthermore, monosomy 7 and 11q23 translocations involving the mixed lineage leukemia (*MLL*) gene are frequently accompanied by deregulated expression of EVI1.[2,4,5] Regardless of cytogenetics, high EVI1 expression predicts adverse outcome mainly due to a poor therapeutic response.[2,4,5,8] In addition to adult AML cases described above, elevated expression of EVI1 is frequently observed in pediatric AML with *MLL* rearrangements and monosomy 7.[9] Importantly, recent reports have suggested

that high EVI1 expression can serve as a poor prognostic indicator in pediatric AML harboring *MLL* rearrangements.[10,11]

Evi1 plays a pivotal role in regulating the self-renewal capacity of hematopoietic stem cells (HSCs) during both fetal and adult hematopoiesis. The number of HSCs in the para-aortic splanchnopleural region is significantly decreased in Evi1-deficient mice, and their long-term repopulation capacity is impaired.[12] Evi1 deletion also leads to severe reduction in fetal liver HSCs along with defective multilineage reconstitution ability.[13] Furthermore, conditional knockout (cKO) of *Evi1* in adult mice results in significant loss of repopulating ability of HSCs.[13] Together with the finding that Evi1 is predominantly expressed in murine HSCs with long-term multilineage repopulating activity,[14] Evi1 works as a key molecule that governs HSC homeostasis. One of the functional features of Evi1 is the direct transcriptional regulation of target genes. So far, several essential molecules involved in the maintenance of HSCs, including Gata2,[12,15] Pbx1,[16] and Pten,[17] have been identified as downstream targets of Evi1. In addition to its DNA-binding capacity, Evi1 physically interacts with transcription factors to repress hematopoietic differentiation. For example, Evi1 inhibits the transcriptional activities of Runx1,[18] PU.1,[19] and Gata1[20] through direct binding, which results in suppression of granulocyte differentiation, myelopoiesis, and erythroid differentiation, respectively. These findings reinforce the important role of Evi1 in proper maintenance of HSCs.

Meanwhile, Evi1 exerts diverse oncogenic functions such as perturbed cell proliferation and anti-apoptotic capacity. For example, Evi1 suppresses the growth-inhibitory effects of transforming growth factor-β by interacting with SMAD3.[21] Evi1 also directly inhibits c-Jun N-terminal kinase to block stress-induced apoptosis.[22] Recent reports have suggested that Evi1 physically interacts with multiple components of the epigenetic machinery, including C-terminal binding protein,[23] histone deacetylases,[24] histone methyltransferases,[25] DNA methyltransferases,[26] and histone acetyltransferases,[27] thus demonstrating a wide variety of roles in gene regulation. Under Evi1-overexpression, Evi1 recruits polycomb repressive complexes to the *PTEN* locus to epigenetically repress *PTEN* transcription, which leads to the activation of AKT/mammalian target of rapamycin (mTOR) signaling in Evi1 leukemia cells.[17] These findings illustrate that deregulation of Evi1 expression and/or function in HSCs causes global epigenetic perturbation to induce leukemogenesis. In addition, several surface molecules that are specifically expressed in Evi1 leukemia cells have been identified. CD52, a lymphocyte marker, is expressed in EVI1-high AML cell lines as well as in patients' samples, and anti-CD52 monoclonal antibody (Alemtuzumab) is effective for killing these cells.[28] Integrin alpha 6 (ITGA6) is shown to be expressed in EVI1-high AML cells and confers drug resistance by enhancing cell adhesion.[29] More recently, GPR56, one of the G protein-coupled receptors, is reported to be involved in the high cell adhesion and anti-apoptotic property of EVI1-high AML

cells.[30] Taken together, AML with enhanced Evi1 expression can be developed and maintained by deregulated transcriptional networks, signaling pathways, and interaction with microenvironments, possibly explaining the poor therapeutic responses to conventional chemotherapy and the high relapse rates.

In this study, I sought to clarify novel molecular features of AML with high Evi1 expression using the mouse model of Evi1 leukemia previously established[17,31] in combination with microarray data analysis. By analyzing gene expression data of AML patients, I first revealed that the expression of *ITGA2B* (CD41), a megakaryocytic differentiation marker, positively correlates with that of *EVI1*. In Evi1 leukemia mice, a subpopulation of leukemia cells did express CD41. Importantly, $CD41^+$ Evi1 leukemia cells had a more efficient leukemia-initiating capacity (LIC) than $CD41^-$ cells. In addition, Mpl, the receptor for thrombopoietin (THPO), was predominantly expressed in the $CD41^+$ cells, and stimulation by THPO supported their growth and survival via upregulation of BCL-xL. These results suggest that the THPO/MPL pathway can be critical for the progression of Evi1 leukemia as a cell-extrinsic factor.

Methods

Vectors

Retroviral vectors used in this study were as follows: pMYs-mouse Evi1-internal ribosome entry site (IRES)-green fluorescent protein (GFP),[17] pMSCV-MLL-ENL-IRES-GFP,[32] pMSCV-neo-Flag-MLL-ENL,[32] and pGCDNsam-MOZ-TIF2-IRES-enhanced GFP.[33] Evi1 cDNA was kindly provided by Dr. Kazuhiro Morishita. MLL-ENL cDNA was a gift from Dr. Ryoichi Ono and Dr. Tetsuya Nosaka. MOZ-TIF2 cDNA was a gift from Dr. Issay Kitabayashi. The pMYs-mouse Evi1-IRES-GFP vector was kindly provided by Dr. Takuro Nakamura. Murine *Evi1* gene used in this study encodes the *Evi1* isoform of *Mds1 and Evi1 complex locus* (*Mecom*), and its sequence information has been registered with the accession number JQ665270.1 in GenBank.

Retroviral transduction

To produce retroviruses, Plat-E packaging cells (kindly provided by Dr. Toshio Kitamura)[34] were transiently transfected with retroviral constructs using Fugene 6 transfection reagent (Roche Applied Science, Basel, Switzerland). Viral supernatants were harvested after 48 hours and added to the culture plate coated with RetroNectin (Takara Bio, Otsu, Japan). Cells were seeded onto the virus-binding plate and infected with retroviruses for 48 hours.

Myeloid transformation

Transformation of primary murine BM cells by Evi1 and MLL-ENL was carried out as described previously.[32] Briefly, for establishing Evi1-immortalized cells, c-kit$^+$ BM mononuclear cells (BM-MNCs) were retrovirally transduced with Evi1-GFP for 48 hours. For producing MLL-ENL-immortalized cells, BM-MNCs isolated from mice treated with 5-fluorouracil (5-FU) were retrovirally transduced with pMSCV-MLL-ENL-IRES-GFP for 48 hours. GFP-positive cells were sorted and cultured in cytokine-supplemented methylcellulose medium (MethoCult GF M3434 from StemCell Technologies, Vancouver, BC, Canada). Colonies were replated in M3434 weekly. After 3 or 4 rounds of replating, immortalized cells were used for subsequent experiments.

Leukemia mouse models

Evi1 leukemia mice were established as described previously.[17,31] In brief, BM-MNCs isolated from C57BL/6 mice after treatment with 5-FU were retrovirally transduced with Evi1. The infected cells were injected through the tail vein into sublethally irradiated (5.25 Gy) syngeneic recipient mice. Generation of MLL-ENL and MOZ-TIF2 leukemia mice was performed as previously reported.[32,33] In brief, BM-MNCs harvested from 5-FU-treated mice were transduced with pMSCV-neo-Flag-MLL-ENL, and transduced cells were transplanted into sublethally irradiated mice. For generation of MOZ-TIF2

leukemia mice, lineage^{-}/c-kit^{+}/Sca-1^{-}/FcγR^{high}/CD34^{+} granulocyte-monocyte progenitors isolated from C57BL/6 mice were transduced with MOZ-TIF2 and transplanted into sublethally irradiated mice. All animal experiments were approved by The University of Tokyo Institutional Animal Care and Use Committee.

Flow cytometry

Cell sorting and analysis were performed by using FACSAriaII, FACSAriaIII, and LSRII (all from BD Biosciences, San Jose, CA). The data were analyzed using FACSDiva software (BD Biosciences) and FlowJo software (Tree Star, Ashland, OR).

Fluorochrome-conjugated antibodies used for staining murine cells were as follows: phycoerythrin (PE) anti-CD41 (BioLegend, San Diego, CA, USA), allophycocyanin (APC) anti-CD41 (eBioscience, San Diego, CA, USA), APC anti-c-kit (BioLegend), PECy7 anti-c-kit (BioLegend), PerCP/Cy5.5 anti-c-kit (BioLegend), PE anti-Gr-1 (BioLegend), APC anti-Gr-1 (BioLegend), APC anti-Mac-1 (BioLegend), APC anti-CD150 (BioLegend), and biotinylated anti-CD150 (BioLegend). The anti-mouse Mpl monoclonal antibody (clone AMM2; provided by Kyowa Hakko Kirin) was labeled with Alexa Fluor 647 using the Alexa Fluor 647 Monoclonal Antibody Labeling Kit (Invitrogen, Carlsbad, CA) according to the manufacturer's instructions. PI (propidium iodide) or DAPI (4',6-diamidino-2-phenylindole) was used to exclude dead cells.

For sorting $CD41^+$ and $CD41^-$ Evi1 leukemia cells, BM- or spleen (SP)-MNCs were stained with an APC anti-CD41 antibody. $CD41^+$ and $CD41^-$ cells within a GFP^+ fraction were sorted and subjected to analysis.

For sorting subfractions of Evi1 leukemia cells, BM-MNCs were stained with PECy7 anti-c-kit, PE anti-CD41, and APC anti-CD150 antibodies. Among c-kit^+ cells in a GFP^+ fraction, 4 subfractions were defined as follows: Fr.1 ($CD41^+/CD150^+$), Fr.2 ($CD41^+/CD150^-$), Fr.3 ($CD41^-/CD150^+$), and Fr.4 ($CD41^-/CD150^-$). These fractions were sorted and subjected to a transplantation assay.

For sorting subfractions of human AML cells, cells were stained with APC anti-CD41, PE anti-CD34, and fluorescein isothiocyanate (FITC) anti-CD38 antibodies (all from BioLegend). 7-AAD (7-aminoactinomycin D) was used to exclude dead cells. $CD34^+/CD41^+$ and $CD34^+/CD41^-$ fractions were sorted and subjected to quantitative real-time polymerase chain reaction (qPCR) analysis. For 1 patient's sample, $CD34^+/CD38^-/CD41^+$, $CD34^+/CD38^-/CD41^-$, $CD34^+/CD38^+/CD41^+$, and $CD34^+/CD38^+/CD41^-$ fractions were sorted.

Limiting dilution transplantation assay

Four subfractions were sorted from secondary Evi1 leukemia BM cells as described above. Cells in each fraction were intravenously injected into sublethally irradiated (5.25 Gy)

mice and monitored for disease development. Incidence of leukemia in mice was evaluated at 20 weeks post-transplantation.

Culture of OP9 cells

OP9 stromal cells obtained from RIKEN Cell Bank (Tsukuba, Japan) were maintained on a gelatin-coated culture dish in α-MEM (Wako Pure Chemical Industries, Osaka, Japan) supplemented with 20% FCS and 1% penicillin-streptomycin.

In vitro culture of leukemia cells

For colony-forming cell assays, $CD41^+$ and $CD41^-$ Evi1 leukemia cells (each 1×10^4) were seeded in MethoCult M3434. After 7 days culture, colonies were counted. For cell proliferation and apoptosis assays, $CD41^+$ and $CD41^-$ Evi1 leukemia cells (each 5×10^4 per well) were seeded onto a confluent layer of OP9 stromal cells in a 24-well plate in the presence of stem cell factor (SCF) (50 ng/mL) and/or THPO (50 ng/mL). The anti-mouse Mpl antibody was added to the culture to block THPO/MPL signaling. Chemical inhibitors used were AG490 (Merck Millipore, Billerica, MA), PD98059 (Cayman Chemical, Ann Arbor, MI), Ly294002 (LC Laboratories, Woburn, MA), and WEHI-539-hydrochloride (ChemScene, Monmouth Junction, NJ). The half of the culture medium was replaced every 2 days. After 7 days culture, cells were harvested by trypsinization and the number of

viable leukemia cells was determined using trypan blue exclusion. Leukemia cells were distinguished from OP9 cells under the microscope by their difference in cell size. For an in vitro cytokine stimulation assay, Evi1 or MLL-ENL leukemia cells were serum-starved in α-MEM containing 1% bovine serum albumin (BSA) at 37°C for 60 minutes. Cells were then suspended in α-MEM containing 0.1% BSA and stimulated with SCF (50 ng/mL) or THPO (50 ng/mL) at 37°C for 60 minutes. Unstimulated controls were also prepared in parallel.

Cell-cycle analysis

Cells were fixed with 70% cold ethanol at 4°C for at least 12 hours and stained with phosphate-buffered saline (PBS) containing 50 μg/mL PI and 250 μg/mL RNaseA at 37°C for 30 minutes. Cell-cycle distribution was analyzed by fluorescence-activated cell sorter (FACS).

Apoptosis analysis

Cells were harvested and suspended in binding buffer (10 mM Hepes [pH 7.5], 140 mM NaCl, and 2.5mM $CaCl_2$) with APC-Annexin V (BD Biosciences). After incubation for 15 minutes in the dark, cell viability was analyzed by FACS. OP9 cells were gated out using forward and side scatter plots.

QPCR

Total RNA was isolated by using RNeasy kit (QIAGEN, Hilden, Germany) or NucleoSpin kit (Takara Bio), and the cDNA was synthesized using SuperScript III reverse transcriptase (Invitrogen) or ReverTra Ace (Toyobo, Osaka, Japan). QPCR was performed by using FastStart SYBR Green Master (Roche Applied Science) or THUNDERBIRD qPCR Mix (Toyobo), with a LightCycler 480 System (Roche Applied Science) according to the manufacturer's instructions. The results were normalized to the expression levels of *18S rRNA* and *GAPDH* for murine and human cells, respectively. PCR primers used were as follows: mEvi1_F, cgaacctaacacggcacttgag; mEvi1_R, ctgcaggttggaagaaatgctg; mItga2b_F, cagccactttggcttctcag; mItga2b_R, acggctccagtctcctcttg; MLL-ENL_F, gtcagaaacctaccccatcag; MLL-ENL_R, gccgagacattcccttctt; mMpl_F, gggcctactgctgctaaagtg; mMpl_R, acccggtgtaggtctggaag; mBcl-xL_F, tgaatgaccacctagagccttg; mBcl-xL_R, tcccgtagagatccacaaaagtg; mBcl-2_F, gaaccggcatctgcacac; mBcl-2_R, catgctggggccatatagttc; mMcl-1_F, cggccttcctcactcctg; mMcl-1_R, tttctccgcaggccaaac; m18SrRNA_F, gactcaacacgggaaacctcac; m18SrRNA_R, atcgctccaccaactaagaacg; hEVI1_F, ccaagtttttcctgatttgcaaagc; hEVI1_R, cctctcttcagtatgtgacagca; hGAPDH_F, acaccatggggaaggtgaag; hGAPDH_R, gtgaccaggcgcccaata.

Western blotting

Cells were lysed with radio-immunoprecipitation assay buffer containing 1 mM sodium vanadate, 1 mM PMSF (phenylmethylsulfonyl fluoride), and complete protease inhibitor cocktail (Roche Applied Science). The lysates were subjected to SDS-PAGE followed by immunoblotting. The primary antibodies used were as follows: anti-STAT3, anti-phospho-STAT3 (Tyr705), anti-ERK1/2, anti-phospho-ERK1/2 (Thr202/Tyr204), anti-AKT, anti-phospho-AKT (Ser473), anti-BCL-xL, anti-BCL-2, anti-MCL-1, and anti-β-Actin antibodies were from Cell Signaling Technology (Danvers, MA, USA); anti-STAT5 and anti-phospho-STAT5 (Tyr694) antibodies were from BD Biosciences. HRP-linked anti-rabbit IgG (Cell Signaling Technology) and HRP-linked anti-mouse IgG (Santa Cruz Biotechnology, Dallas, TX) were used as secondary antibodies. Proteins were detected by ImmunoStar LD (Wako Pure Chemical Industries) with a LAS-4000 system (Fujifilm, Tokyo, Japan). Densitometric quantification was performed using ImageJ software (http://rsbweb.nih.gov/ij).

Microarray data analysis

Gene expression data of 461 human individuals with AML were obtained from Gene Expression Omnibus (GEO; www.ncbi.nlm.nih.gov/geo, accession number GSE6891).[35] The raw data of the 460 samples available were processed and normalized using the

Microarray Analysis Suite 5.0 algorithm (Affymetrix, Santa Clara, CA). Samples were arranged in order of mean expression values of 3 *MDS1 and EVI1 complex locus* (*MECOM*) probes (probe ID: 215851_at, 221884_at, and 226420_at). Top 30 samples were defined as the *EVI1*-high group according to diagnostic information about *EVI1* positivity attached to each data file. Differentially expressed probe sets between the *EVI1*-high group (30 cases) and the *EVI1*-low group (430 cases) were determined by fold change (FC) > 1.4 and $P < .05$, and 573 probes highly expressed in the *EVI1*-high group were extracted. These probe IDs were converted into official gene symbols (400 genes) using DAVID database (http://david.abcc.ncifcrf.gov). For revealing functional gene signatures in the *EVI1*-high group, gene set enrichment analyses (GSEA) was performed with GSEA version 2.0 software available from the Broad Institute (http://www.broad.mit.edu/gsea). All curated gene sets (C2) were utilized for analysis. Ratio of classes was applied as metric for ranking genes and the data permutations were performed 1,000 times. Differences were considered statistically significant at nominal *P* value < .05.

For analyzing another set of human AML microarray data, gene expression data of 422 AML cases were utilized.[36] The data normalized were obtained from GEO (accession number GSE37642; Platform GPL96). Samples were arranged in order of mean expression values of 2 *MECOM* probes (probe ID: 215851_at and 221884_at), and then

divided into the *EVI1*-high group (n = 42) and the *EVI1*-low group (n = 380) based on a provisional threshold of 90 percentile. Differentially expressed probe sets between 2 groups were determined by FC > 1.4 and $P < .05$, and 177 probes highly expressed in the *EVI1*-high group were extracted. These probe IDs were converted into official gene symbols (144 genes) using DAVID database.

Gene expression data of murine c-kit^{+}/Sca-1^{+}/lineage^{-} cells (referred to as KSL) derived from *Evi1* wild-type and cKO mice were analyzed.[13] The data normalized were obtained from the GEO database (accession number GSE11557). Differentially expressed probe sets between KSL derived from *Evi1* cKO mice (n = 2) and that derived from *Evi1* wild-type mice (n = 2) were determined by FC > 1.4 and $P < .05$, and 1844 probes downregulated by *Evi1* deletion were extracted. These probe IDs were converted into official gene symbols (2199 genes) using DAVID database.

To further identify genes highly associated with Evi1 expression, common genes were extracted from 2 gene sets described above: 400 genes highly expressed in the *EVI1*-high AML group (GSE6891) and 2199 genes repressed by *Evi1* deletion (GSE11557). The list of 42 candidate genes, including 11 cell-surface molecules, is shown in Table 1.

Table 1. The list of 42 candidate genes highly correlating with *EVI1* expression identified by combined analysis of human AML microarray (GSE6891) and *Evi1* cKO mice microarray (GSE11557) data

Symbol	Official gene name	Probe ID	FC
ABAT	4-aminobutyrate aminotransferase	224098_at	1.435
ABCA1*	ATP-binding cassette, sub-family A (ABC1), member 1	203504_s_at	1.513
ARHGAP6	Rho GTPase activating protein 6	206167_s_at	1.470
ATF7IP	activating transcription factor 7 interacting protein	216197_at	1.428
BCL11A	B-cell CLL/lymphoma 11A (zinc finger protein)	1559078_at	1.607
		222891_s_at	1.412
BCL2	B-cell CLL/lymphoma 2	232614_at	1.539
BEX2	brain expressed X-linked 2	224367_at	1.877
CMTM8*	CKLF-like MARVEL transmembrane domain containing 8	235099_at	1.618
COL18A1	collagen, type XVIII, alpha 1	209081_s_at	1.799
DACH1	dachshund homolog 1 (Drosophila)	1567101_at	3.060
		228915_at	1.979
		205471_s_at	1.939
		1562342_at	1.915
		205472_s_at	1.717
EFHC2	EF-hand domain (C-terminal) containing 2	220591_s_at	2.241
GPR56*	G protein-coupled receptor 56	212070_at	1.839
		206582_s_at	1.679
HES1	hairy and enhancer of split 1, (Drosophila)	203395_s_at	1.401
HTR1F*	5-hydroxytryptamine (serotonin) receptor 1F	221458_at	2.119
ITGA2B*†	integrin, alpha 2b (platelet glycoprotein IIb of IIb/IIIa complex, antigen CD41)	206494_s_at	2.573
		216956_s_at	1.812
		206493_at	1.806
ITGB3*†	integrin, beta 3 (platelet glycoprotein IIIa, antigen CD61)	204627_s_at	1.970
		204625_s_at	1.438
ITPR3	inositol 1,4,5-triphosphate receptor, type 3	201189_s_at	1.415
KRT18	keratin 18	201596_x_at	2.002
LTBP3	latent transforming growth factor beta binding protein 3	219922_s_at	1.827
MMRN1	multimerin 1	205612_at	4.701
MPL*†	myeloproliferative leukemia virus oncogene	207550_at	1.404
MYLK	myosin light chain kinase	224823_at	2.488
		202555_s_at	1.567

NFIA	nuclear factor I/A	224970_at	1.801
		224975_at	1.786
		232997_at	1.457
NRN1*	neuritin 1	218625_at	1.867
NXN	nucleoredoxin	219489_s_at	1.465
OBSL1	obscurin-like 1	212775_at	1.424
PEAR1*†	platelet endothelial aggregation receptor 1	228618_at	1.944
PELI1	pellino homolog 1 (Drosophila)	232213_at	1.571
		232304_at	1.529
PFKM	phosphofructokinase, muscle	210976_s_at	1.543
PTK2	PTK2 protein tyrosine kinase 2	208820_at	1.444
PTPRD*	protein tyrosine phosphatase, receptor type, D	213362_at	2.679
		214043_at	2.514
		205712_at	1.685
RAB27B	RAB27B, member RAS oncogene family	207018_s_at	1.428
RBM38	RNA binding motif protein 38	212430_at	1.409
RBMS3	RNA binding motif, single stranded interacting protein	238447_at	1.422
RFTN1	raftlin, lipid raft linker 1	242672_at	1.426
RUNX3	runt-related transcription factor 3	204198_s_at	1.465
		204197_s_at	1.455
SELP*†	selectin P (granule membrane protein 140kDa, antigen CD62)	206049_at	1.495
SMAD3	SMAD family member 3	239448_at	1.511
SOCS2	suppressor of cytokine signaling 2	203372_s_at	2.411
		203373_at	2.316
SPOCK2	sparc/osteonectin, cwcv and kazal-like domains proteoglycan	202524_s_at	1.425
SSBP2	single-stranded DNA binding protein 2	1557813_at	1.587
		1561690_at	1.505
		1557814_a_at	1.433
ZBTB46	zinc finger and BTB domain containing 46	227329_at	1.735

FCs calculated from the microarray data of human AML samples are shown.

* These genes represent cell-surface marker genes.

† These genes represent surface markers of megakaryocyte and platelet lineage.

Short hairpin RNA-mediated knockdown of Mpl

A target sequence for Mpl short hairpin RNA (shRNA) was identified by using Clontech RNAi Target Sequence Selector. The oligonucleotides encoding Mpl shRNA and control shRNA were cloned into the pSIREN-RetroQ retroviral vector (Takara Bio) according to the manufacturer's instructions. BM cells derived from Evi1 leukemia mice were precultured in α-MEM supplemented with 20% FCS, 1% penicillin-streptomycin and cytokines (40 ng/mL SCF, 10 ng/mL IL-3, 20 ng/mL IL-6, 20 ng/mL THPO, and 20 ng/mL Flt3 ligand) and subjected to retroviral infection as described above. After 48 hours of culture, cells were collected and further cultured in fresh medium containing 1.5 μg/mL puromycin for 72 hours. Puromycin-resistant cells were used for BM transplantation assays. The target sequences were as follows: Mpl, CAGTGACAATTGGACTTCA; control, AAATGTACTGCGTGGAGAC.

Human samples

A total of 4 BM cells derived from patients with AML were obtained from the Department of Hematology and Oncology of The University of Tokyo Hospital. The study was approved by the ethics committee of The University of Tokyo, and written informed consent in accordance with the Declaration of Helsinki was obtained from all patients whose samples were collected.

Statistics

The data were analyzed by Student *t* test, Tukey's test, or Dunnett's test. Differences were considered statistically significant at $P < .05$. To analyze the survival curve, the log-rank test was used. LIC frequency was calculated by Poisson statistics. Data analysis was performed using R software (http://www.R-project.org).

Results

Expression of *ITGA2B* correlates with that of *EVI1* in human AML

First, I analyzed 2 sets of microarray data and identified 42 genes that were highly associated with *EVI1* expression, including 11 cell-surface molecules (Figure 1A and Table 1). The reason for focusing on cell-surface molecules is that these surface markers enable the separation of cell populations and comparison of their leukemic properties in both Evi1 leukemia mice and in human AML subjects. These candidate cell-surface molecules included several megakaryocyte/platelet lineage markers such as *ITGA2B* (CD41), *ITGB3* (CD61), *PEAR1*, *SELP*, and *MPL*. Analysis of another set of AML microarray data[36] confirmed that the expression of *ITGA2B*, *MPL*, and *SELP* was correlated with that of *EVI1* (Table 2). In addition, GSEA revealed that molecular signatures relevant to platelet function and integrin αIIbβ3 (CD41/CD61) signaling were significantly enriched in the *EVI1*-high group (Figure 1B–E). These results indicate that the expression of megakaryocytic markers, in particular *ITGA2B*, strongly correlates with that of *EVI1* in human AML.

Expression levels of candidate megakaryocytic marker genes were comparable between *EVI1*-high cases with 3q abnormalities and those without 3q abnormalities (Figure 2A). When compared with *MLL*-rearranged cases without *EVI1* expression, those with *EVI1* overexpression showed higher expression of *ITGA2B*, *MPL*, and *PEAR1* (Figure

2B). These results suggested that expression of megakaryocytic marker genes would mark *EVI1*-positive AML cases irrespective of cytogenetic abnormalities.

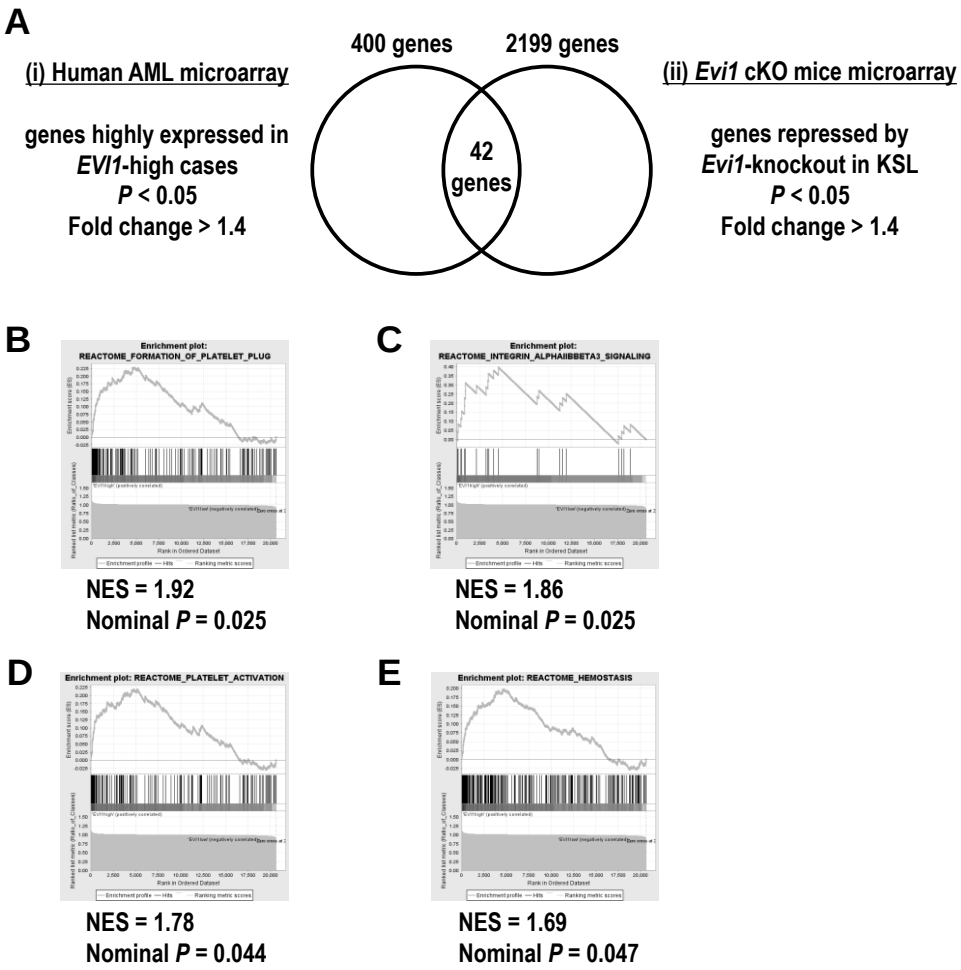

Figure 1. Genes expressed in the megakaryocyte and platelet lineage correlate with *EVI1* expression.

(A) The candidate genes positively correlated with *EVI1* expression were extracted by analyzing 2 different sets of microarray data: (i) human AML BM specimens (GSE6891) and (ii) KSL cells derived from *Evi1* cKO mice (GSE11557). For human AML microarray analysis, samples were divided into *EVI1*-high AML (30 cases) and *EVI1*-low AML (430 cases) groups according to *EVI1* expression as well as diagnostic information, and then 400 genes highly expressed in the *EVI1*-high AML group were identified (FC > 1.4 and P < .05). From *Evi1* cKO mice microarray data, 2199 genes downregulated by *Evi1*-knockout in KSL cells were extracted (FC > 1.4 and P < .05). The Venn diagram revealed that 42 genes were highly correlated with *EVI1* expression. (B–E) According to the GSEA, several gene sets related to platelet function were enriched in the *EVI1*-high AML group compared with the *EVI1*-low AML group. (B) Gene set name, REACTOME_FORMATION_OF_PLATELET_PLUG; 174 genes. (C) Gene set name, REACTOME_INTEGRIN_ALPHAIIBBETA3_SIGNALING; 23 genes. (D) Gene set name, REACTOME_PLATELET_ACTIVATION; 155 genes. (E) Gene set name, REACTOME_HEMOSTASIS; 262 genes. NES indicates the normalized enrichment score.

Table 2. The list of 144 genes highly correlating with *EVI1* expression in another set of human AML microarray data (GSE37642)

ABCA1	ABLIM1	ACOX2	ALDH1A1	ANGPT1	ARHGAP6	ARMCX1	ASAP2
C1orf54	CD1D	CD300A	CD48	CD52	CD7	CHRDL1	CLEC2B
CNN3	COL5A1	CRABP1	CRIM1	CSF1	DACH1	DBNDD2	DCHS1
DSG2	DUSP7	DZIP1	EFHC2	EGR3	EPS8	ERG	ETV5
FAM30A	FCER1A	FEZ1	FHL2	FRMD4B	FZD6	FZD7	GALNT12
GJA1	GNAI1	GP1BB	GPR126	GPR56	GPRC5C	GUCY1B3	H2AFY
HOPX	HOXA10	HOXA11	HPGD	HTR1F	ID4	IGHG1	IL12RB2
IL7	INHBA	INPP4B	IPW	ITGA2B	ITGA6	KDELC1	KIAA0125
KRT18P19	LAG3	LGALS1	LMO4	LOC100134230	LOC731884	LOX	LRBA
LST1	LTBP3	MAF	MECOM	MEF2C	MEIS1	MFAP3L	MICAL1
MLLT3	MMRN1	MN1	MPL	MPPED2	MS4A2	MYL9	MYO6
NAP1L3	NGFRAP1	NPDC1	NRIP1	NRXN2	NYNRIN	OBSL1	PAWR
PCDH9	PDLIM2	PDLIM5	PLCB4	PLEKHA5	PLS3	PRDX1	PRKACB
PRKCH	PRKCZ	PRKD3	PRR16	RBM47	RBP4	RBPMS	SCD
SDPR	SELP	SENP6	SERPINE2	SERPING1	SH3BP4	SH3BP5	SMAD7
SNRPN	SOCS2	SPAG6	SPP1	TCF7L2	TIE1	TIMP3	TKTL1
TNFSF10	TNNT1	TOX	TPBG	TPM2	TRPM4	TRPS1	TSPAN4
VWA5A	VWF	WBP5	WHAMML1	XAF1	XAGE1B	ZEB1	ZNF232

Genes colored in gray are commonly found in Table 1.

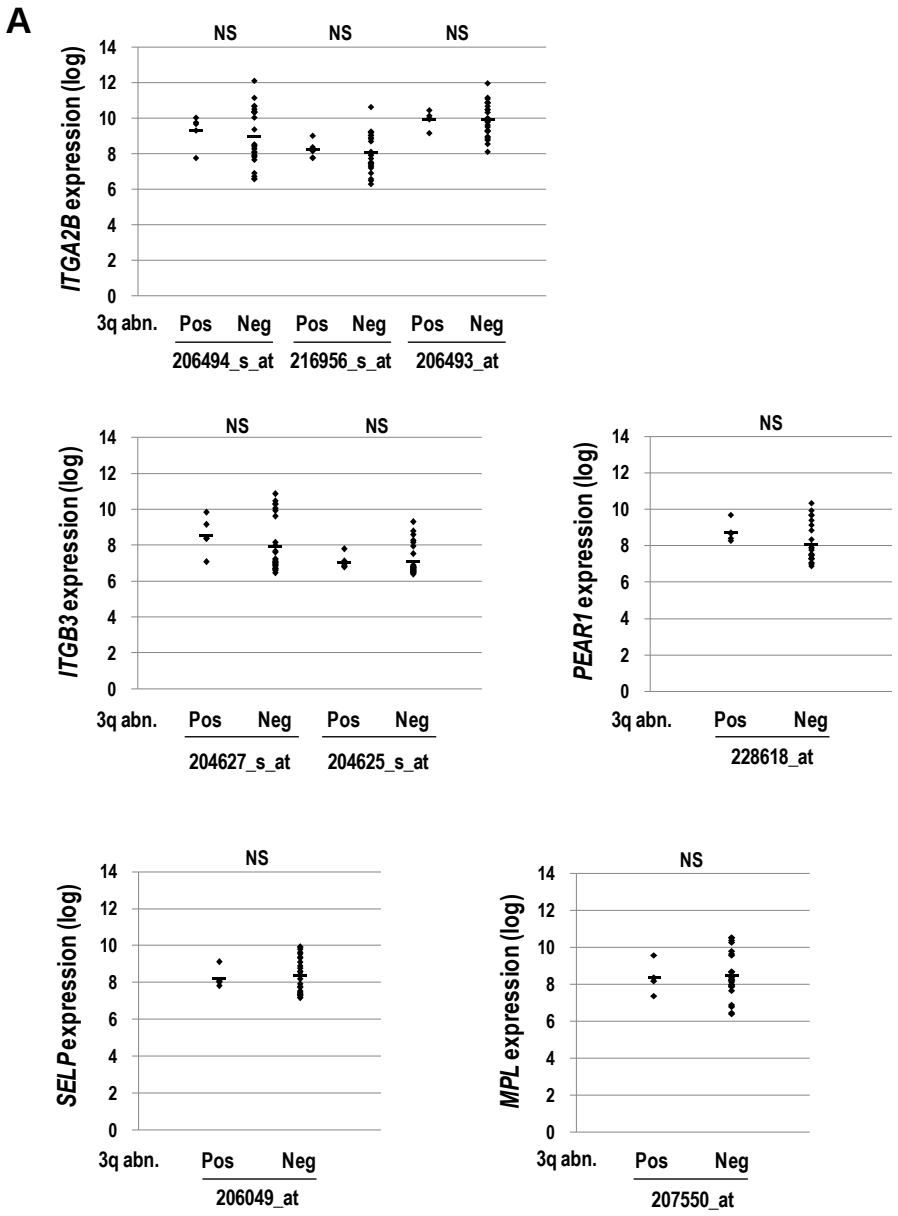

Figure 2. Comparison of expression levels of megakaryocytic surface marker genes by human AML microarray data analysis.

(A) Comparison of gene expression levels between *EVI1*-high cases with 3q abnormalities (n = 5) and those without 3q abnormalities (n = 25) (GSE6891). The expression levels of *ITGA2B*, *ITGB3*, *PEAR1*, *SELP*, and *MPL* were comparable irrespective of the presence of 3q abnormalities (NS means not significant; Student *t* test). All probe IDs examined are described in Table 1.

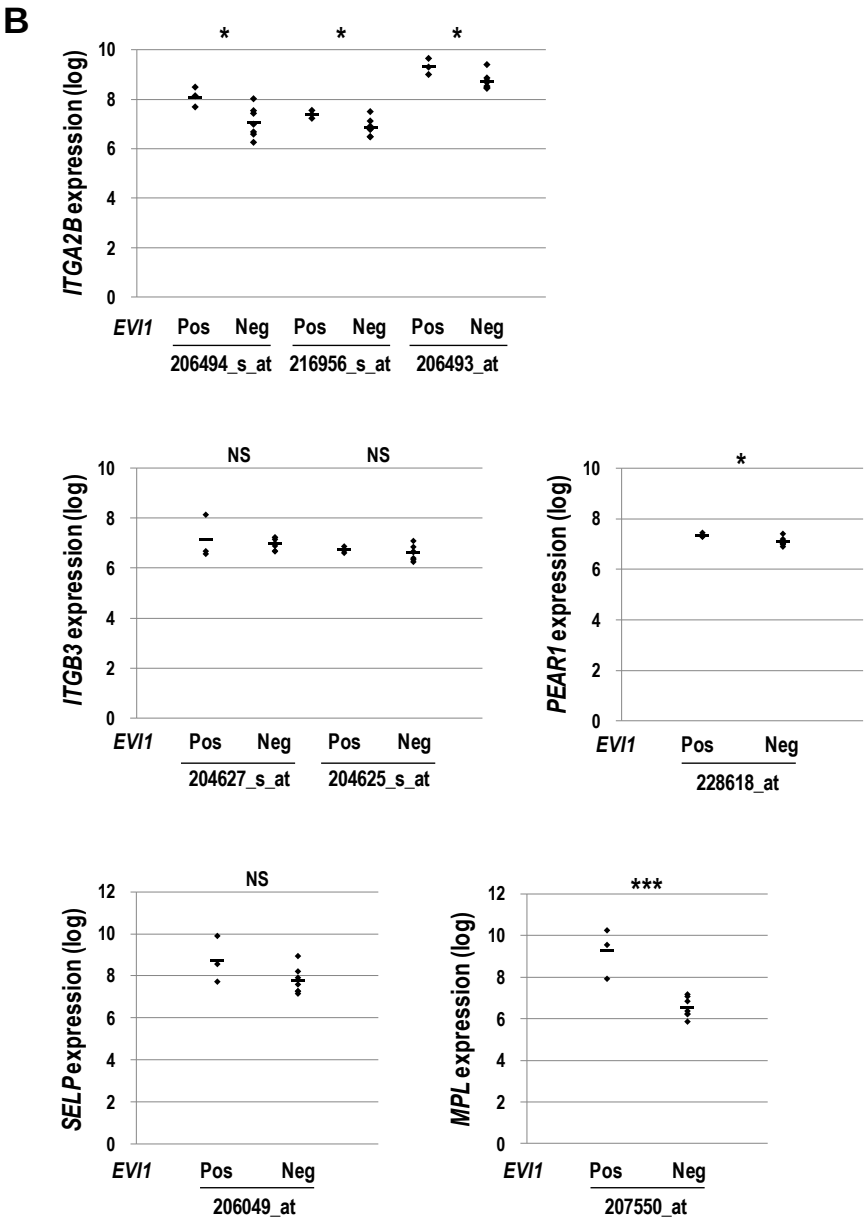

Figure 2. Comparison of expression levels of megakaryocytic surface marker genes by human AML microarray data analysis. (continued)

(B) Comparison of gene expression levels between *EVI1*-positive *MLL*-rearranged cases (n = 3) and *EVI1*-negative *MLL*-rearranged cases (n = 7) (GSE6891). Among genes examined, the expression levels of *ITGA2B*, *PEAR1*, and *MPL* in *EVI1*-positive *MLL*-rearranged cases were higher than those in *EVI1*-negative *MLL*-rearranged cases (**P* < .05, ****P* < .001, Student *t* test).

Evi1-overexpressing cells express CD41

To confirm the association between CD41 and Evi1, I next examined CD41 expression in hematopoietic cells immortalized by Evi1. Murine c-kit$^+$ BM cells were transduced with Evi1-GFP or mock-GFP retroviral vectors, and GFP$^+$ cells were sorted and subjected to qPCR and FACS analysis (Figure 3A). *Itga2b* expression was increased 1.5-fold by Evi1 overexpression 2 days after transduction (Figure 3B). After 3 rounds of replating in semisolid culture, transformed Evi1-GFP$^+$ cells clearly expressed CD41 (Figure 3C). To exclude the possibility that immortalized CD41$^+$ cells are generated exclusively from the CD41$^+$ normal BM cells transduced with Evi1, CD41$^-$ BM cells were purified and transduced with Evi1 (Figure 4A). Even in this setting, Evi1 overexpression induced CD41$^+$ immortalized cells (Figure 4B). I next examined CD41 expression in MLL-ENL-transduced murine BM cells in which Evi1 expression can be upregulated.[32] BM cells from 5-FU-treated mice were transduced with MLL-ENL and immortalized in a semisolid culture. In this way, I obtained 2 *Evi1*-positive and 2 *Evi1*-negative clones (Figure 5A). The expression levels of the *MLL-ENL* transgene were comparable among these clones, except in 1 *Evi1*-positive clone in which *MLL-ENL* expression was approximately 2 times higher than that of the others. As described in a previous report, efficient Evi1-upregulation is observed when immature KSL cells rather than BM progenitor cells are transduced with MLL-ENL.[32] The fact that Evi1-positivity differed

among 4 clones might reflect a difference in 5-FU-primed BM cell populations transformed by MLL-ENL in each experiment. Although upregulation of *Evi1* was relatively mild compared with the forced expression, the $Evi1^{+}$ clones clearly showed higher expression of *Itga2b* than the $Evi1^{-}$ clones and expressed CD41 (Figure 5B–C). These results demonstrate that CD41 expression is accompanied by Evi1 expression in mouse BM cells immortalized in vitro.

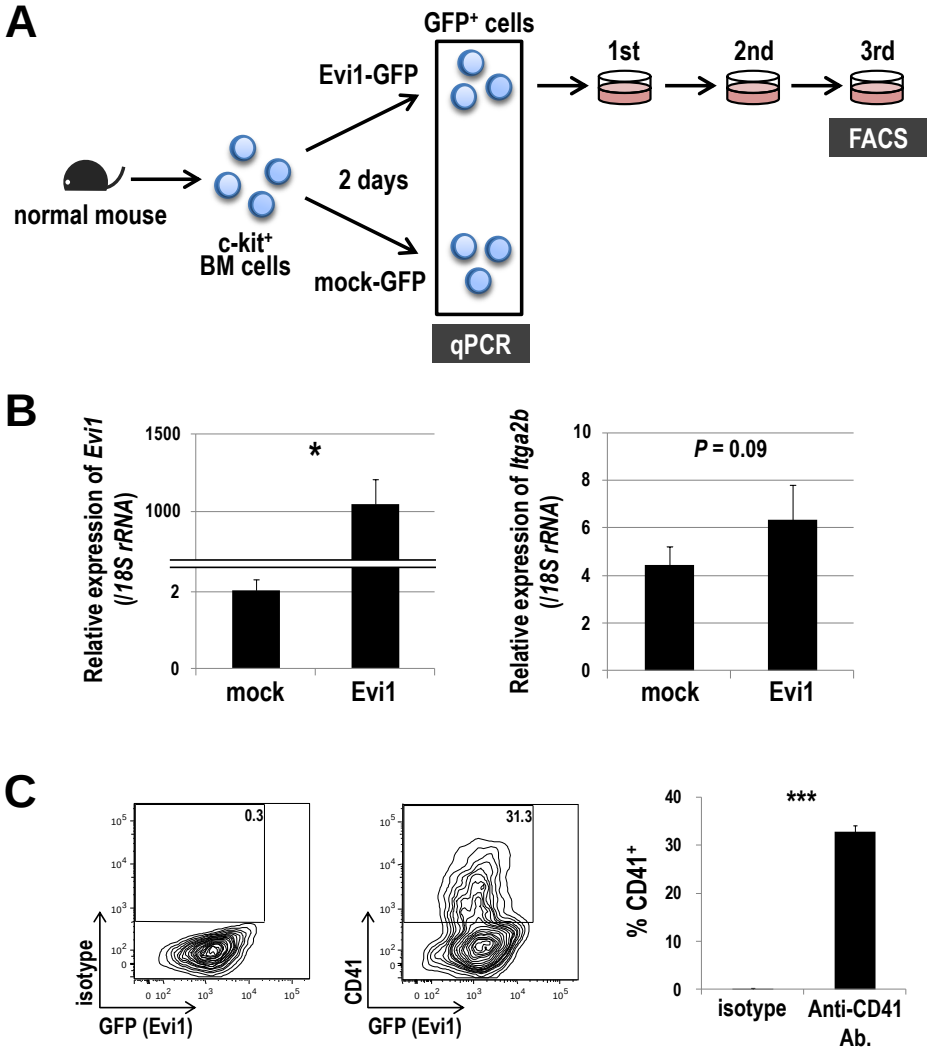

Figure 3. Evi1-overexpressing cells express CD41.

(A) Schematic representation of gene expression and FACS analysis. Murine c-kit$^+$ BM cells were transduced with Evi1-GFP or mock-GFP for 2 days, and GFP$^+$ cells were sorted and subjected to gene expression analysis. Evi1-GFP-transduced cells were seeded in cytokine-supplemented methylcellulose culture medium (MethoCult M3434) and serially replated. FACS analysis was performed at the third replating. Three independent experiments were performed. (B) The messenger RNA (mRNA) expression of *Evi1* (left) and *Itga2b* (right) was compared between Evi1-GFP- and mock-GFP-transduced murine BM cells. Expression levels relative to normal c-kit$^+$ BM cells are presented. Error bars indicate standard deviation (SD; n = 3; **P* < .05, Student *t* test). (C) Surface CD41 expression was analyzed by FACS. Cells were stained with a PE-conjugated isotype control antibody or a PE-conjugated anti-CD41 antibody. Representative FACS data and a bar graph showing frequencies of CD41$^+$ cells are presented. Error bars indicate SD (n = 3; ****P* < .001, Student *t* test).

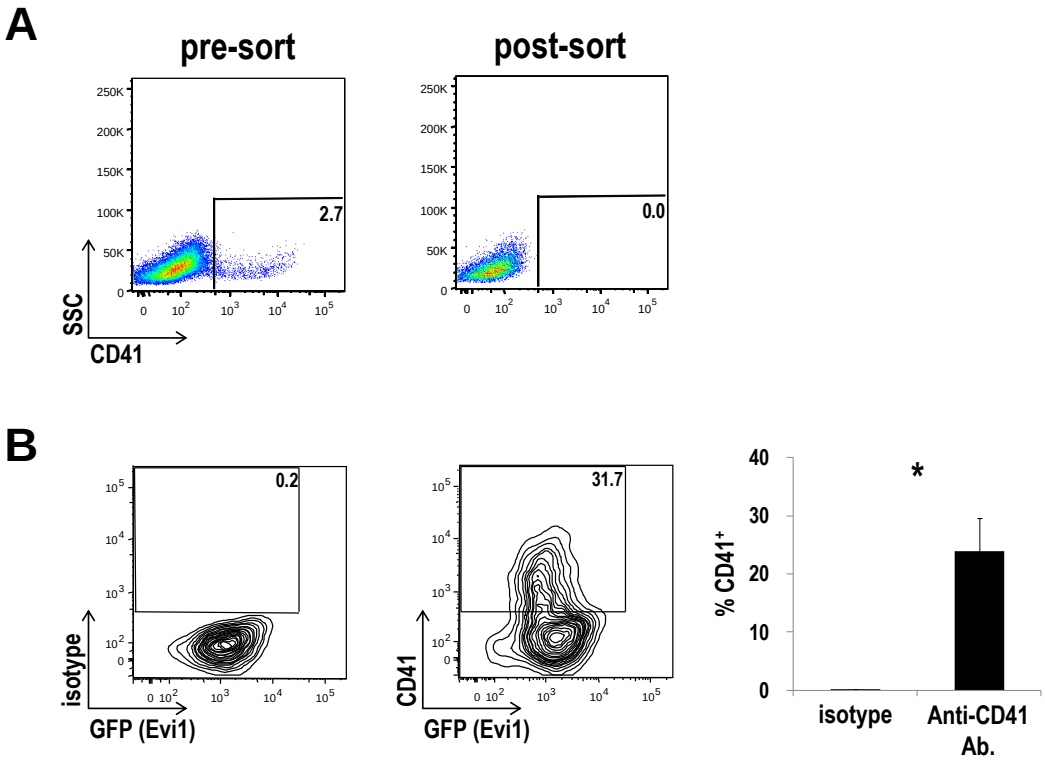

Figure 4. CD41$^+$ immortalized cells are generated from CD41$^-$ normal BM cells transduced with Evi1.

(A) Murine c-kit$^+$ BM-MNCs contained a small fraction of CD41$^+$ cells (pre-sort). The CD41$^+$ cells were completely depleted by cell sorting (post-sort). (B) Purified CD41$^-$ cells were retrovirally transduced with Evi1-GFP for 2 days. GFP$^+$ cells were isolated by FACS and seeded onto MethoCult M3434. The surface expression of CD41 was analyzed by FACS at the third replating. Representative FACS data and a bar graph showing frequencies of CD41$^+$ cells are presented. Error bars indicate SD (n = 3; *P < .05, Student t test).

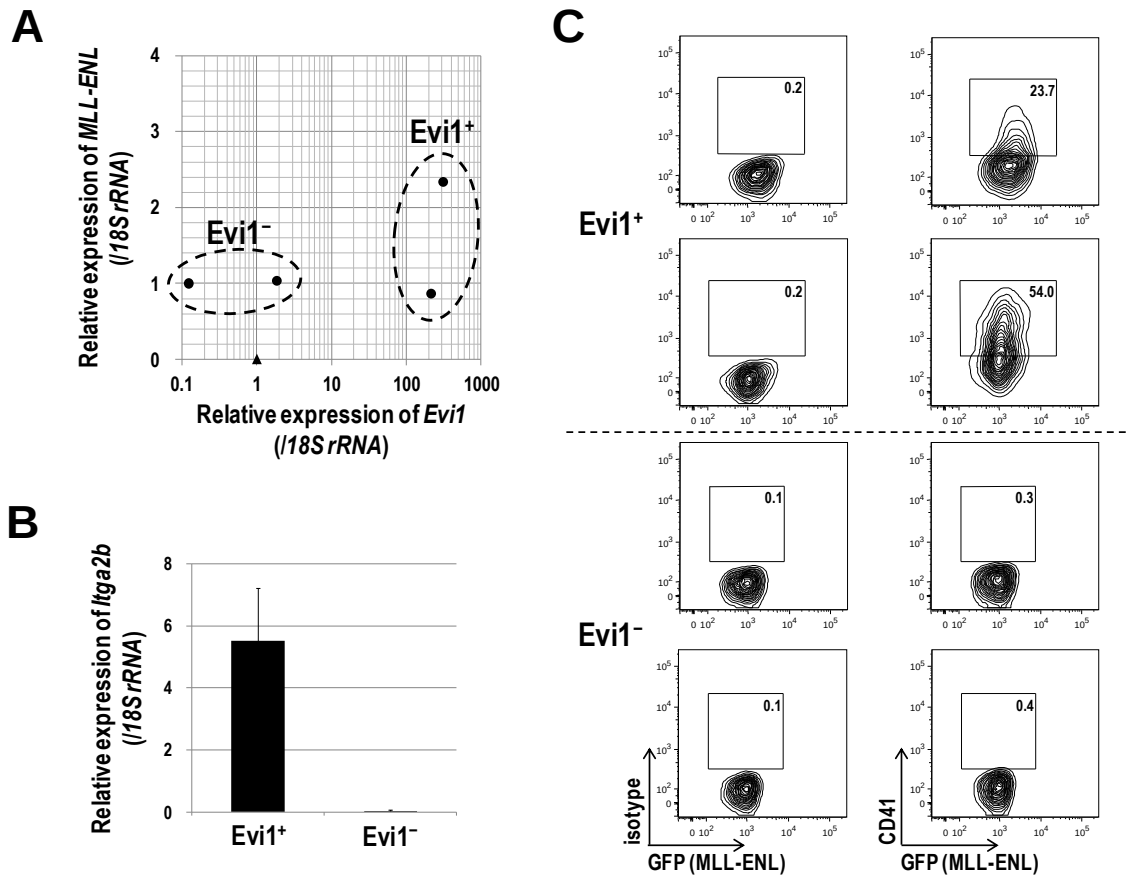

Figure 5. Evi1$^+$ MLL-ENL-immortalized cells express CD41.

(A) BM-MNCs isolated from 5-FU-treated mice were retrovirally transduced with MLL-ENL and immortalized by serially replating in semisolid culture. Four MLL-ENL-immortalized clones from 2 independent experiments were established. The mRNA expression levels of *Evi1* (x-axis) and *MLL-ENL* (y-axis) are shown. Obviously, 4 MLL-ENL-transduced clones (closed circles) are divided into Evi1$^+$ (n = 2) and Evi1$^-$ (n = 2) clones as indicated. A closed triangle indicates normal c-kit$^+$ BM cells. (B) Comparison of *Itga2b* expression levels between Evi1$^+$ and Evi1$^-$ clones. Expression levels relative to normal c-kit$^+$ BM cells are presented. Error bars indicate SD. (C) Surface CD41 expression was analyzed by FACS. Evi1$^+$ clones, but not Evi1$^-$ clones, clearly expressed CD41.

CD41$^+$ Evi1 leukemia cells have a higher LIC than CD41$^-$ cells

Next, I checked CD41 expression in the mouse model of Evi1 leukemia.[17,31] As shown in Figure 6A, CD41 was distinctly expressed in BM and SP cells of Evi1 leukemia mice. CD41$^+$ cells expressed immature markers such as c-kit and CD150 more frequently than CD41$^-$ cells (Figure 6B). In contrast, Gr-1- and Mac-1-positive mature cells were frequently present in the CD41$^-$ fraction. I then postulated that CD41$^+$ cells mark a phenotypically and functionally immature fraction of Evi1 leukemia mice and contain subfraction(s) with a higher LIC. Both CD41$^+$ and CD41$^-$ cells within a GFP$^+$, namely, Evi1$^+$ fraction were sorted and subjected to further analysis (Figure 7A). Morphological analysis revealed that CD41$^+$ cells contained myeloblasts with high nucleus/cytoplasm ratio more abundantly than CD41$^-$ cells (Figure 7B). In a colony-forming assay, CD41$^+$ cells generated larger colonies and showed higher colony-forming capacity than CD41$^-$ cells (Figure 8A). There was no significant difference between CD41$^+$ and CD41$^-$ cells in the cell-cycle status (Figure 8B). On the other hand, apoptotic rates were significantly lower in CD41$^+$ cells than in CD41$^-$ cells (Figure 8C). Next, I performed secondary BM transplantation assays, wherein mice received CD41$^+$ or CD41$^-$ cells developed AML characterized by the emergence of large numbers of myeloblasts as observed in primary leukemia mice (Figure 6–7) along with marked splenomegaly (data not shown). Importantly, the mice transplanted with CD41$^+$ cells died from AML more rapidly than

those transplanted with $CD41^-$ cells (Figure 9). Expression profiles of CD41 in secondary leukemia mice were similar to those in primary leukemia mice (data not shown). Given that the significant difference of homing capacity between $CD41^+$ and $CD41^-$ cells was not observed 12 hours after transplantation, delayed onset of AML in mice transplanted with $CD41^-$ cells might not due to its impaired homing capacity (Figure 10). To further define subpopulation(s) with a high LIC, 4 subfractions were classified based on CD41 and CD150 expression patterns within GFP^+/$c\text{-}kit^+$ cells and transplanted into mice (Figure 11A). A limiting dilution transplantation assay revealed that 3 fractions other than the $c\text{-}kit^+/CD41^-/CD150^-$ fraction (Fr.4) showed extremely high LIC frequencies (Figure 11B). These results demonstrated that $c\text{-}kit^+/CD41^-/CD150^+$ (Fr.3) as well as $c\text{-}kit^+/CD41^+$ (Fr.1 and Fr.2) cells marked a LIC within Evi1 leukemia cells.

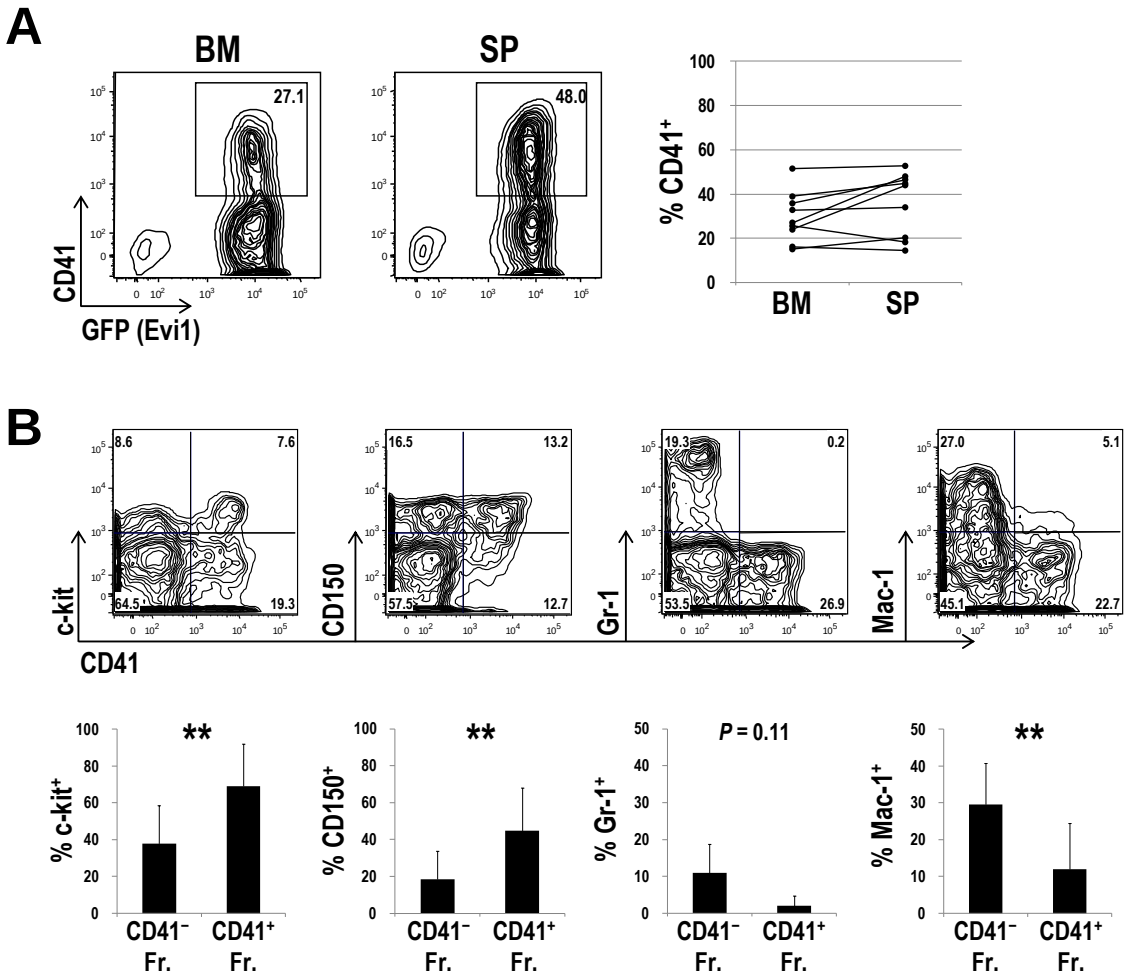

Figure 6. CD41 is expressed in BM and SP cells derived from Evi1 leukemia mice.
(A) The surface expression of CD41 on Evi1 leukemia cells. BM- and SP-MNCs were harvested from Evi1 leukemia mice, and stained with an APC-conjugated anti-CD41 antibody. Representative FACS data are shown. The graph shows frequencies of $CD41^+$ cells in BM and SP derived from 9 individual leukemia mice. (B) Surface-marker profiles of Evi1 leukemia BM cells. Cells were stained with a PE-conjugated anti-CD41 antibody and APC-conjugated antibodies (c-kit, CD150, Gr-1, or Mac-1). Data for GFP^+ cells are shown. Bar graphs show frequencies of $c\text{-}kit^+$, $CD150^+$, $Gr\text{-}1^+$, and $Mac\text{-}1^+$ cells in $CD41^+$ and $CD41^-$ fractions. Error bars indicate SD (n = 5; $^{**}P < .01$, Student *t* test).

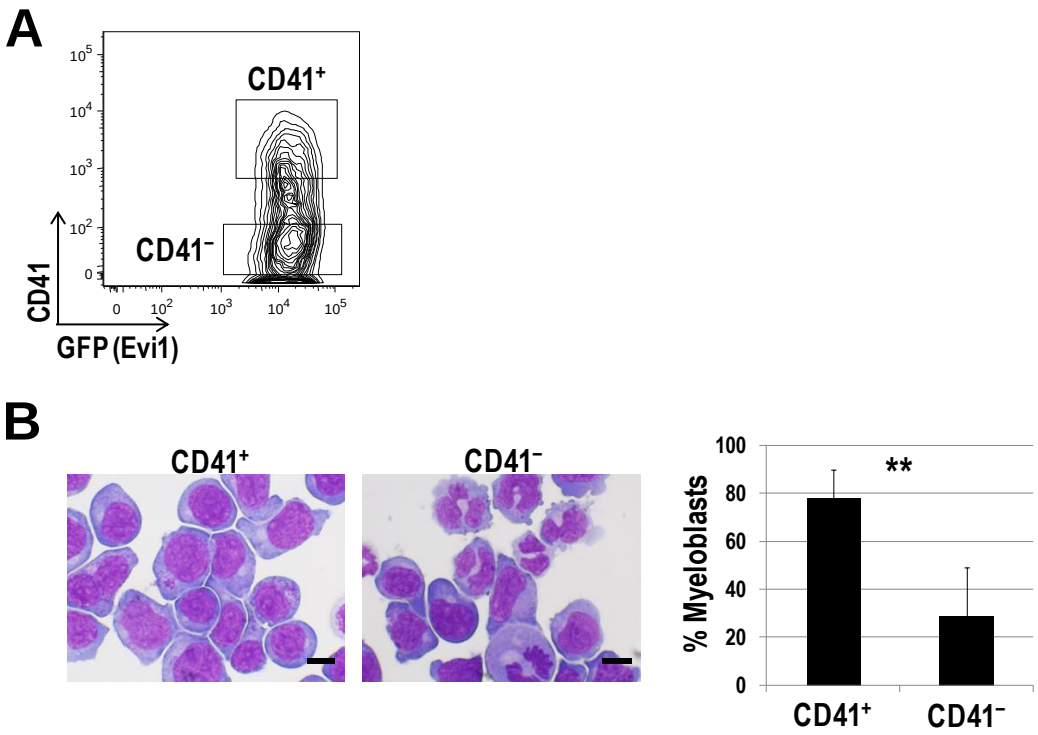

Figure 7. CD41$^+$ Evi1 leukemia cells are morphologically more immature cells than CD41$^-$ cells.

(A) CD41$^+$ and CD41$^-$ Evi1 leukemia cells within a GFP$^+$ fraction were sorted and subjected to further analysis. A representative FACS plot is shown. (B) The morphological feature of CD41$^+$ and CD41$^-$ cells was examined by Wright-Giemsa staining, and the proportion of myeloblasts with a high nucleus/cytoplasm ratio was compared between these fractions. Pictures were captured by a BH-2 microscope equipped with an NC SPlan objective lens and a DP20 camera module (both from Olympus, Tokyo, Japan). Scale bars represent 10 μm. Error bars indicate SD (n = 5; $^{**}P < .01$, Student *t* test).

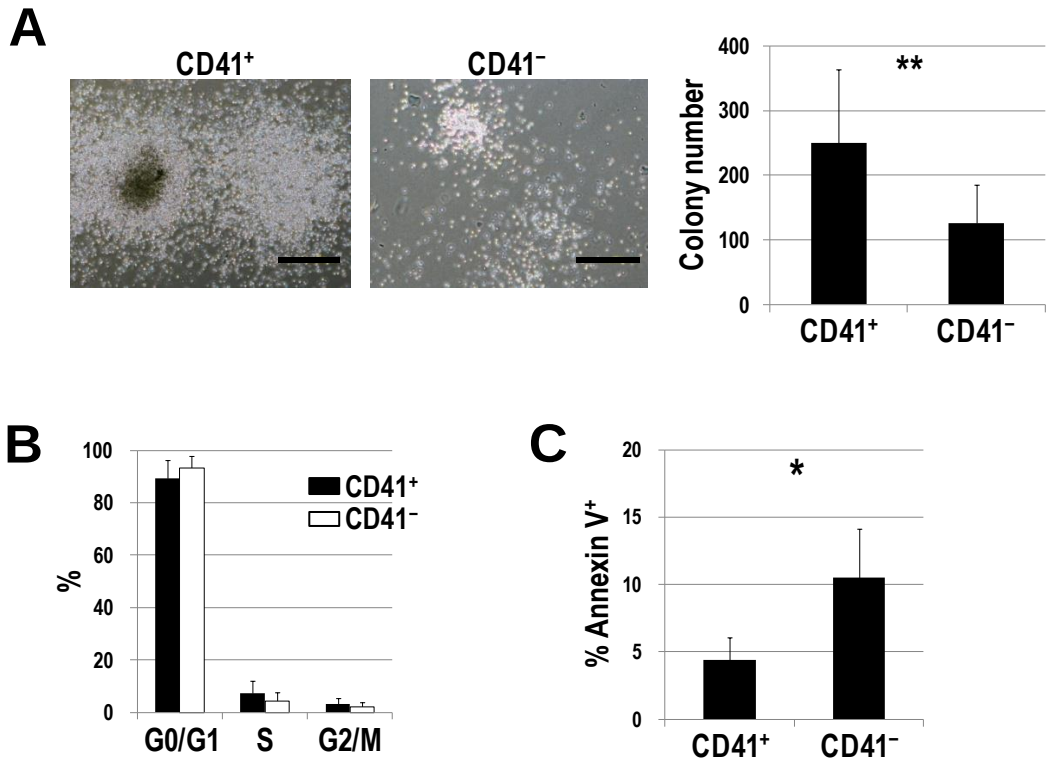

Figure 8. CD41$^+$ Evi1 leukemia cells show higher colony-forming capacity and a lower apoptotic rate than CD41$^-$ cells.

(A) CD41$^+$ and CD41$^-$ cells were cultured in MethoCult M3434 medium and examined their colony-forming activities. Representative pictures of colonies and a bar graph showing colony numbers from each fraction are presented. Scale bars represent 500 μm. Error bars indicate SD (n = 8; $^{**}P < .01$, Student *t* test). (B) The cell-cycle status of CD41$^+$ and CD41$^-$ cells was analyzed by PI staining. Error bars indicate SD (n = 3). (C) Apoptosis analysis of CD41$^+$ and CD41$^-$ cells. Freshly isolated BM-MNCs were stained with a PE-conjugated anti-CD41 antibody, followed by staining with APC-conjugated Annexin V. Apoptotic rates in CD41$^+$ and CD41$^-$ fractions were determined by FACS. Error bars indicate SD (n = 4; $^{*}P < .05$, Student *t* test).

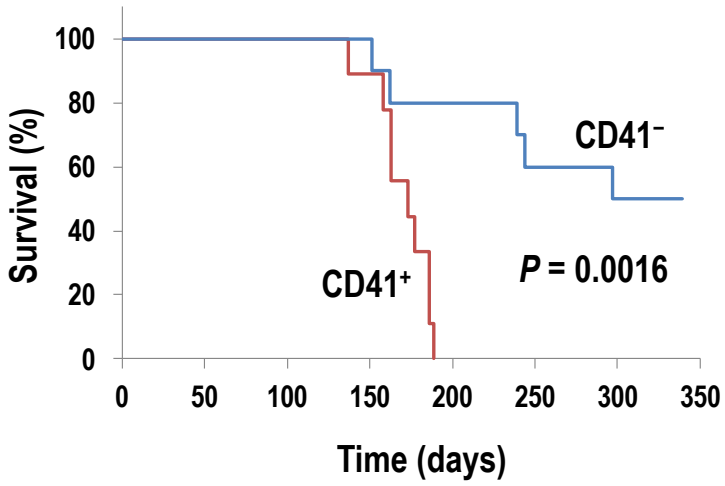

Figure 9. CD41$^+$ Evi1 leukemia cells have a higher LIC than CD41$^-$ cells.
CD41$^+$ and CD41$^-$ fractions were sorted from primary Evi1 leukemia BM cells and intravenously injected into sublethally irradiated (5.25 Gy) mice (1×10^4 cells per mouse). Survival curves of mice transplanted with CD41$^+$ (n = 9; red line) or CD41$^-$ (n = 10; blue line) Evi1 leukemia cells are shown (P = .0016, log-rank test).

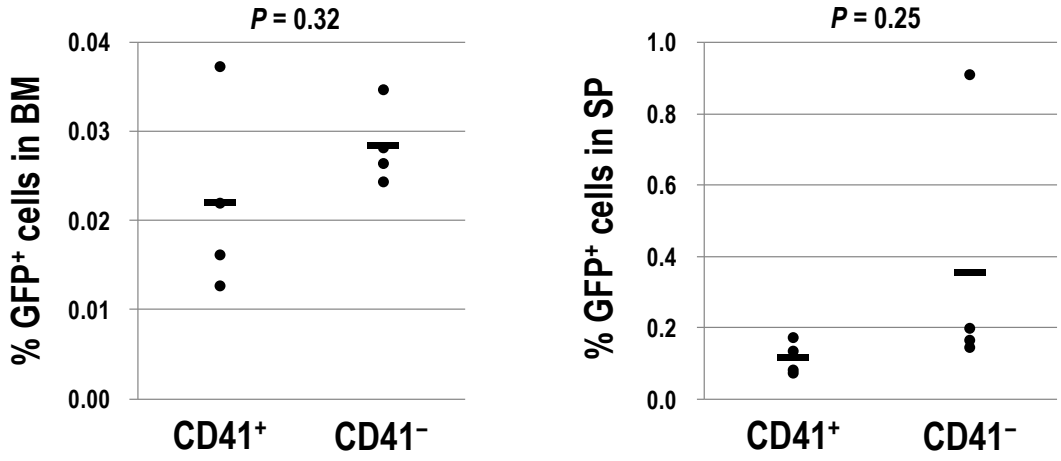

Figure 10. Comparison of homing capacity between CD41$^+$ and CD41$^-$ Evi1 leukemia cells.

CD41$^+$ or CD41$^-$ cells sorted from secondary Evi1 leukemia BM cells were transplanted into sublethally irradiated mice (4.5×10^5 cells per mouse; n = 4 each). BM- and SP-MNCs were harvested 12 hours after transplantation, and frequencies of GFP$^+$ cells in BM (left) and SP (right) were analyzed by FACS. The significant difference of homing capacity between these fractions was not observed (Student *t* test).

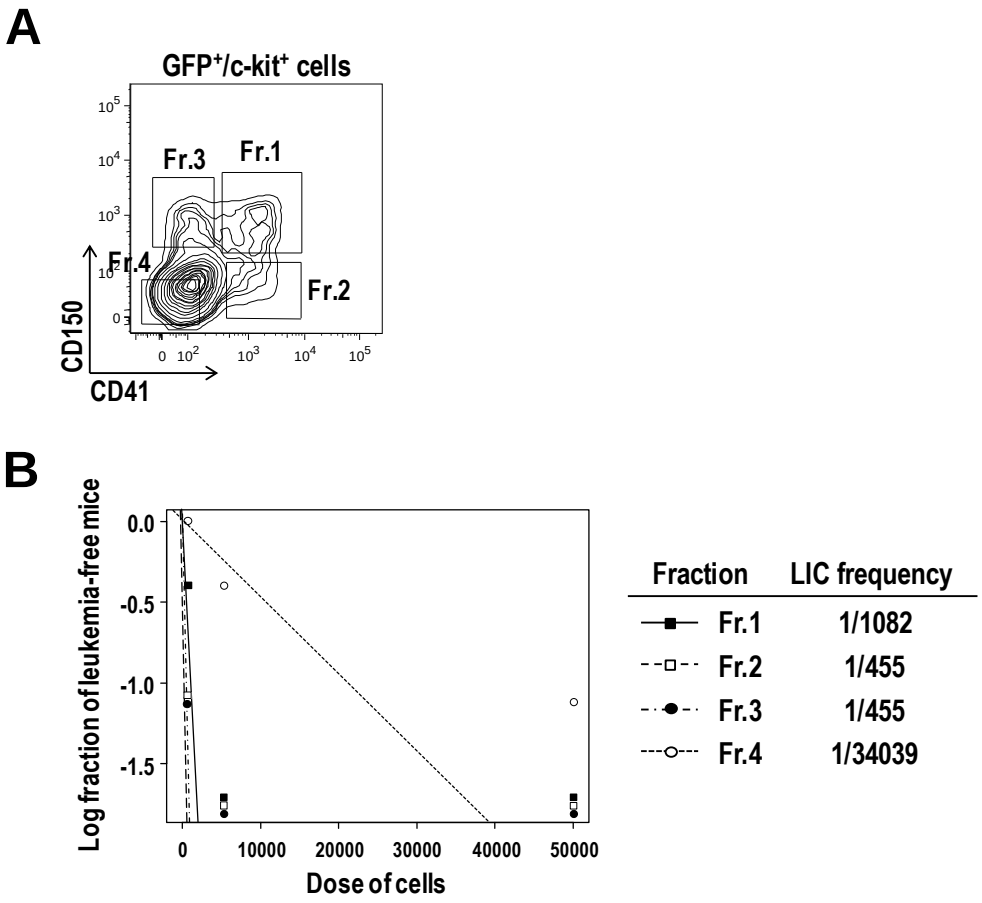

Figure 11. Comparison of LIC frequencies in the 4 subfractions of Evi1 leukemia cells.

(A) The GFP^+/c-kit^+ fraction in Evi1 leukemia BM cells was divided into 4 subfractions: Fr.1 ($CD41^+/CD150^+$), Fr.2 ($CD41^+/CD150^-$), Fr.3 ($CD41^-/CD150^+$), and Fr.4 ($CD41^-/CD150^-$). (B) LIC frequencies in each fraction as determined by a limiting dilution transplantation assay are shown. See Table 3 for detailed transplantation results.

Table 3. Limiting dilution transplantation assay data

Cell population	Transplanted cells	Incidence of leukemia (%)
Fr.1	50000	3/3 (100)
	5000	3/3 (100)
	500	1/3 (33)
Fr.2	50000	3/3 (100)
	5000	3/3 (100)
	500	2/3 (66)
Fr.3	50000	3/3 (100)
	5000	3/3 (100)
	500	2/3 (66)
Fr.4	50000	2/3 (66)
	5000	1/3 (33)
	500	0/3 (0)

Mpl is predominantly expressed in CD41$^+$ Evi1 leukemia cells

As shown in Table 1 and 2, expression of several megakaryocytic markers correlated with that of *EVI1*. Because Mpl, the THPO receptor, is known as a well-defined molecule, I next tested whether Evi1 leukemia cells express Mpl. As shown in Figure 12A, CD41$^+$ cells showed significantly higher *Mpl* expression than CD41$^-$ cells. FACS analysis confirmed that Mpl was mainly expressed in the CD41$^+$ BM and SP cells (Figure 12B–C). I also assessed Mpl expression in other mouse models of myeloid leukemia induced by MLL-ENL and MOZ-TIF2 oncogenes. Our previous study showed that *Evi1* expression in MLL-ENL leukemia mice varied among individuals,[32] and MLL-ENL leukemia cells used here expressed low levels of *Evi1* (Figure 13A). *Evi1* expression was not detected in MOZ-TIF2 leukemia cells. These leukemia cells expressed neither Mpl nor CD41 (Figure 13B–C).

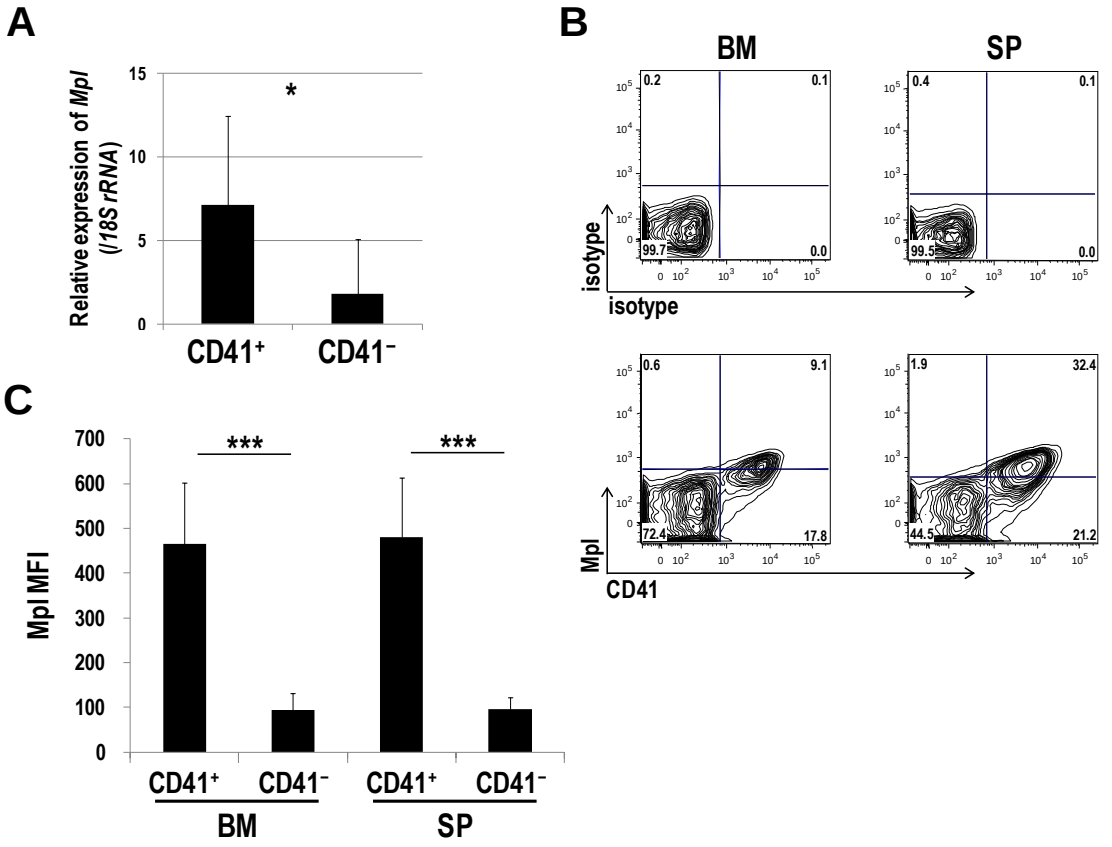

Figure 12. Mpl is predominantly expressed in CD41$^+$ Evi1 leukemia cells.

(A) *Mpl* expression was measured by qPCR in CD41$^+$ and CD41$^-$ BM cells of Evi1 leukemia mice. BM-MNCs were harvested from 5 independent mice and CD41$^+$ and CD41$^-$ cells were sorted. Expression levels relative to normal c-kit$^+$ BM cells are presented. Error bars indicate SD (*P < .05, Student t test). (B–C) FACS analysis of CD41 and Mpl expression in BM- and SP-MNCs from Evi1 leukemia mice. (B) Cells were stained with PE-conjugated anti-CD41 and Alexa Fluor 647-labeled anti-mouse Mpl antibodies. Expression profiles were analyzed for GFP$^+$ cells. (C) Mean fluorescence intensity (MFI) of Mpl was quantified in CD41$^+$ and CD41$^-$ cells. Error bars indicate SD (n = 8; ***P < .001, Student t test).

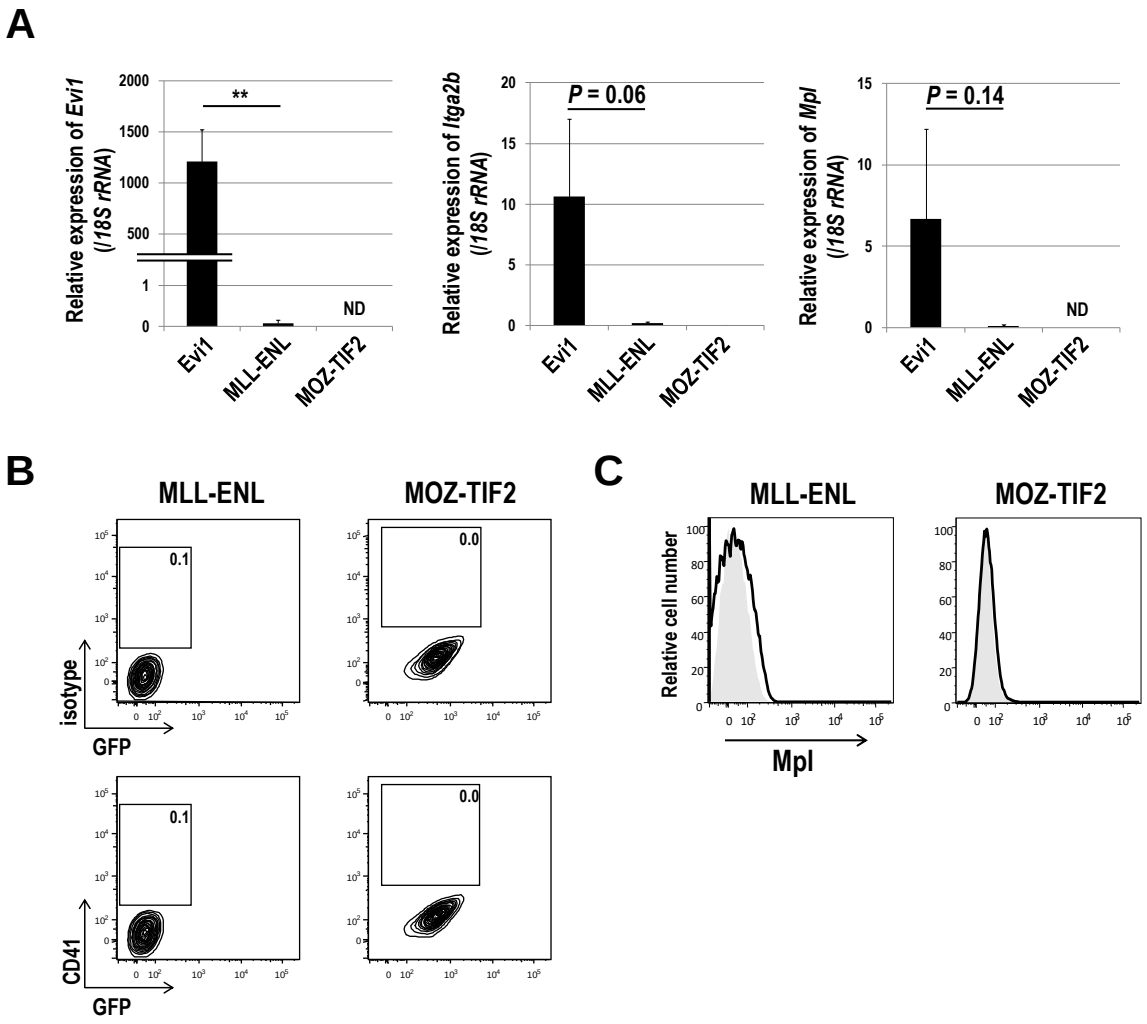

Figure 13. Expression of CD41 and Mpl is not induced in other mouse models of myeloid leukemia.

(A) The expression levels of *Evi1* (left), *Itga2b* (middle), and *Mpl* (right) were measured by qPCR for murine leukemia BM cells induced by Evi1, MLL-ENL, or MOZ-TIF2. Expression levels relative to normal c-kit^{+} BM cells are presented. Error bars indicate SD (Evi1, n = 4; MLL-ENL, n = 3; MOZ-TIF2, n = 2; ND means not detected; $^{**}P < .01$, Student *t* test). (B) SP-MNCs from MLL-ENL leukemia mice and BM-MNCs from MOZ-TIF2 leukemia mice were stained with an APC-conjugated isotype control antibody (upper panel) or an APC-conjugated anti-CD41 antibody (lower panel), and analyzed by FACS. Representative FACS data are shown. (C) SP-MNCs from MLL-ENL leukemia mice and BM-MNCs from MOZ-TIF2 leukemia mice were stained with an Alexa Fluor 647-labeled anti-mouse Mpl antibody. Representative FACS data are shown (solid line, anti-Mpl antibody; filled histogram, isotype control).

THPO/MPL signaling enhances the growth and survival of CD41$^+$ Evi1 leukemia cells

In the hematopoietic system, THPO plays an important role not only in regulating megakaryocytic development and platelet production but also in maintaining quiescent HSCs in the osteoblastic niche.[37,38] Therefore, I next examined effects of THPO on CD41$^+$ and CD41$^-$ Evi1 leukemia cells cultured on OP9 stromal cells. THPO but not SCF more efficiently stimulated the proliferation of CD41$^+$ cells than CD41$^-$ cells (Figure 14A), which correlated well with the expression pattern of Mpl in these fractions. Moreover, the combination of THPO and SCF did not show any synergistic effect on cell growth, indicating that THPO is sufficient for the growth of CD41$^+$ cells. Because CD41$^+$ and CD41$^-$ cells produced each other to some extent during the culture on OP9 cells (data not shown), the clear effect of THPO on CD41$^+$ cells might be masked by the gradual appearance of CD41$^-$ cells. An anti-Mpl neutralizing antibody, AMM2,[38] distinctly inhibited the THPO-mediated growth of CD41$^+$ cells but not CD41$^-$ cells (Figure 14B–C). In addition, CD41$^+$ cells showed a significantly lower apoptotic rate than CD41$^-$ cells in the presence of THPO (Figure 14D). When CD41$^+$ cells were cultured on OP9 feeder cells with or without THPO for 3 days, expression of Gr-1 and Mac-1 was not induced even in the absence of THPO (Figure 15), indicating that THPO might not inhibit differentiation of Evi1 leukemia cells. These results demonstrate that THPO/MPL signaling supports the proliferation and suppresses the apoptosis of the CD41$^+$ Evi1 leukemia cells.

Upon THPO binding, MPL activates several intracellular signals including Janus kinase (JAK)/signal transducer and activator of transcription (STAT), mitogen-activated protein kinase kinase (MEK)/extracellular signal-regulated kinase (ERK), and phosphatidylinositol 3-kinase (PI3K)/AKT pathways. As shown in Figure 16A, STAT3, STAT5, and ERK1/2 were markedly phosphorylated in Evi1 leukemia cells stimulated with THPO but not SCF. In contrast, remarkable phosphorylation of AKT was not induced. Neither THPO nor SCF induced phosphorylation of these molecules in MLL-ENL leukemia cells that did not express Mpl (Figure 16B). When $CD41^+$ cells were treated with a JAK2 inhibitor (AG490) or an MEK inhibitor (PD98059), the number of viable cells decreased by approximately 50% compared with those treated with a vehicle control (Figure 17A). Furthermore, apoptotic cells increased more than 2-fold by addition of AG490 or PD98059 (Figure 17B). Similarly, a PI3K inhibitor, Ly294002, seemed to suppress the growth and induce apoptosis of $CD41^+$ cells (Figure 18), indicating that the PI3K/AKT pathway was actually activated in $CD41^+$ cells. These results demonstrate that JAK/STAT and MEK/ERK pathways are responsible for the growth-accelerating and anti-apoptotic effects of THPO on $CD41^+$ Evi1 leukemia cells.

To test whether THPO/MPL signaling is important for the progression of Evi1 leukemia in vivo, I constructed a shRNA-expressing retroviral vector targeting *Mpl*, by which Mpl^+ Evi1 leukemia cells decreased by about 50% (Figure 19A). Survival analysis

revealed that shRNA-mediated knockdown of Mpl in Evi1 leukemia BM cells partially, but significantly, prolonged the survival of Evi1 leukemia mice (Figure 19B).

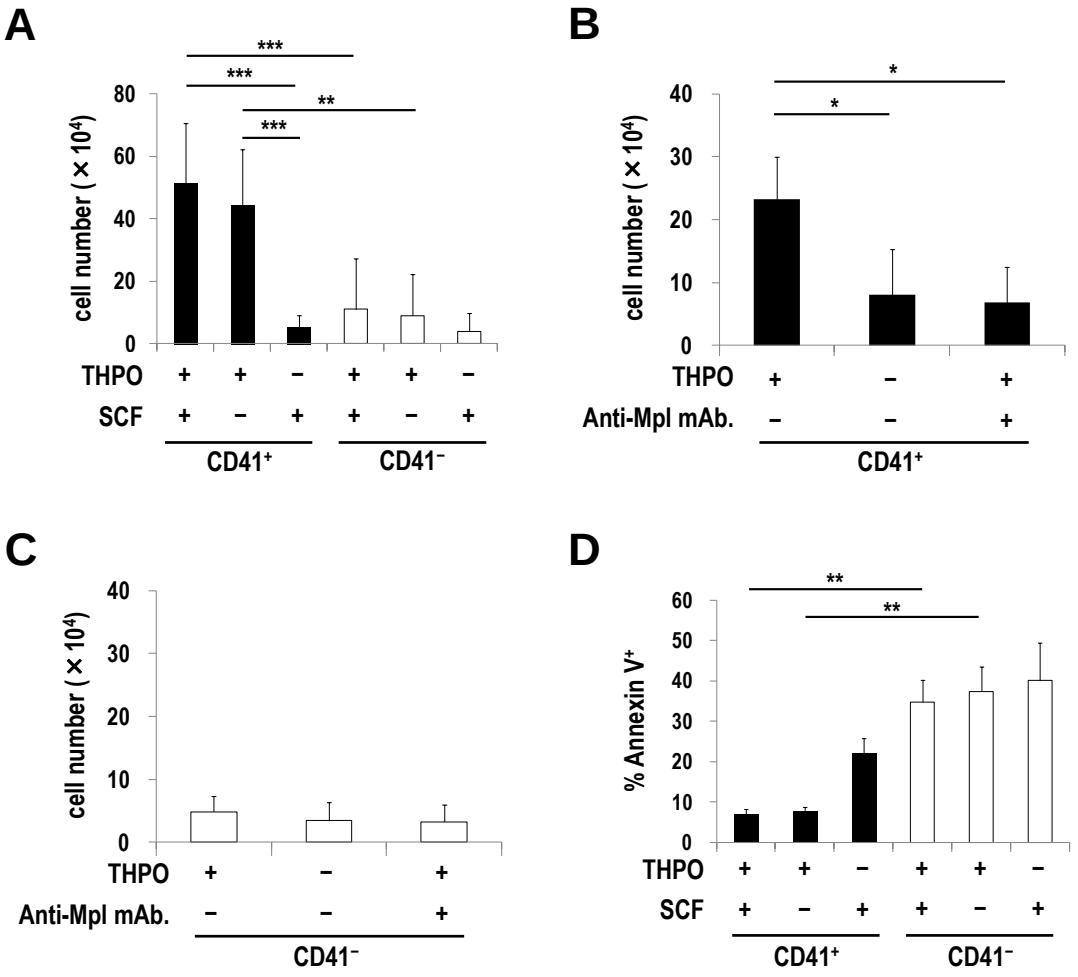

Figure 14. THPO/MPL signaling enhances the growth and survival of CD41$^+$ Evi1 leukemia cells.

(A) Proliferation assays of CD41$^+$ and CD41$^-$ BM cells from Evi1 leukemia mice using OP9 coculture system. CD41$^+$ or CD41$^-$ cells (5×10^4 cells per well) were seeded onto a confluent layer of OP9 stromal cells in the presence of SCF and THPO, THPO alone, or SCF alone. After 7 days of culture, cells were harvested by trypsinization and the number of viable leukemia cells was counted. Error bars indicate SD (n = 7; ***P* < .01, ****P* < .001, Tukey's test). (B–C) The antiproliferation effect of an anti-Mpl antibody against CD41$^+$ cells. CD41$^+$ (B; n = 4) or CD41$^-$ (C; n = 3) cells were seeded onto OP9 stromal cells with or without THPO, or THPO with an anti-Mpl antibody (100 ng/mL) and cultured for 7 days. The number of viable cells was determined as described in panel A. Error bars indicate SD (**P* < .05, Dunnett's test). (D) Apoptosis analysis of CD41$^+$ and CD41$^-$ cells cocultured with OP9 cells. CD41$^+$ or CD41$^-$ cells were cultured in the same condition as panel A. After 7 days culture, cells were harvested and stained with Annexin V, followed by FACS analysis. Error bars indicate SD (n = 3; ***P* < .01, Tukey's test).

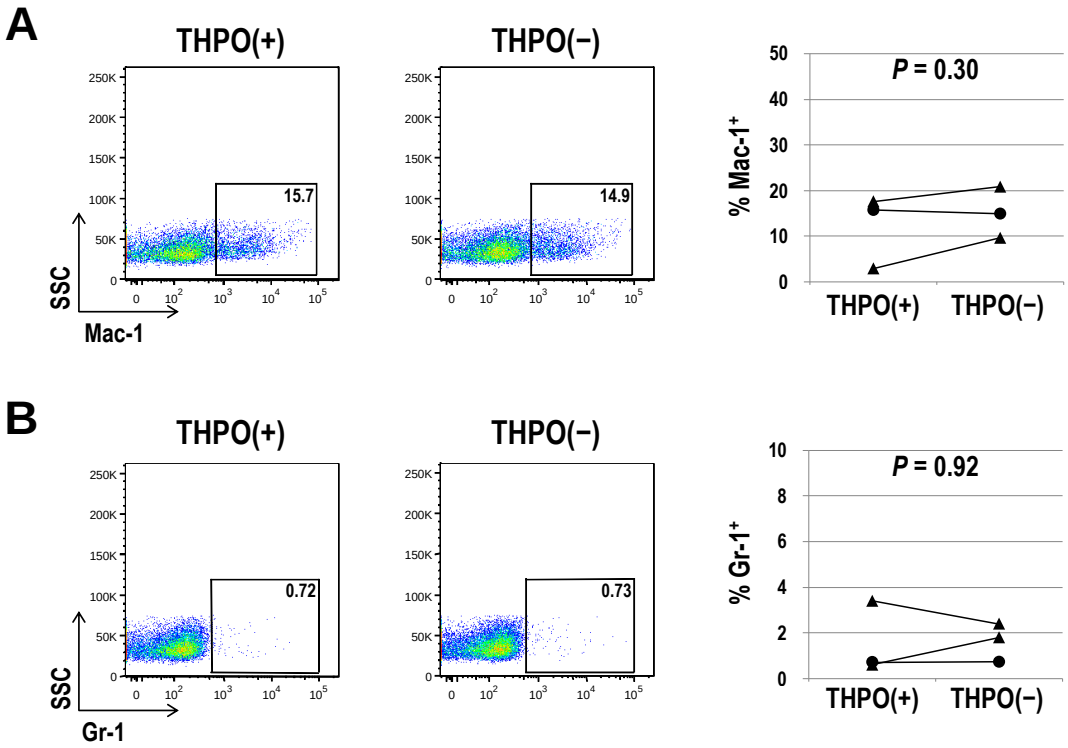

Figure 15. THPO does not inhibit differentiation of CD41$^+$ Evi1 leukemia cells cultured on OP9 stromal cells.

CD41$^+$ Evi1 leukemia BM or SP cells were cultured on OP9 stromal cells with or without THPO for 3 days, and then expression patterns of Mac-1 (A) and Gr-1 (B) were analyzed by FACS. Representative FACS plots are shown. Graphs show the frequencies of Mac-1$^+$ or Gr-1$^+$ cells in each condition. The significant difference in frequencies was not observed (n = 3; Student *t* test).

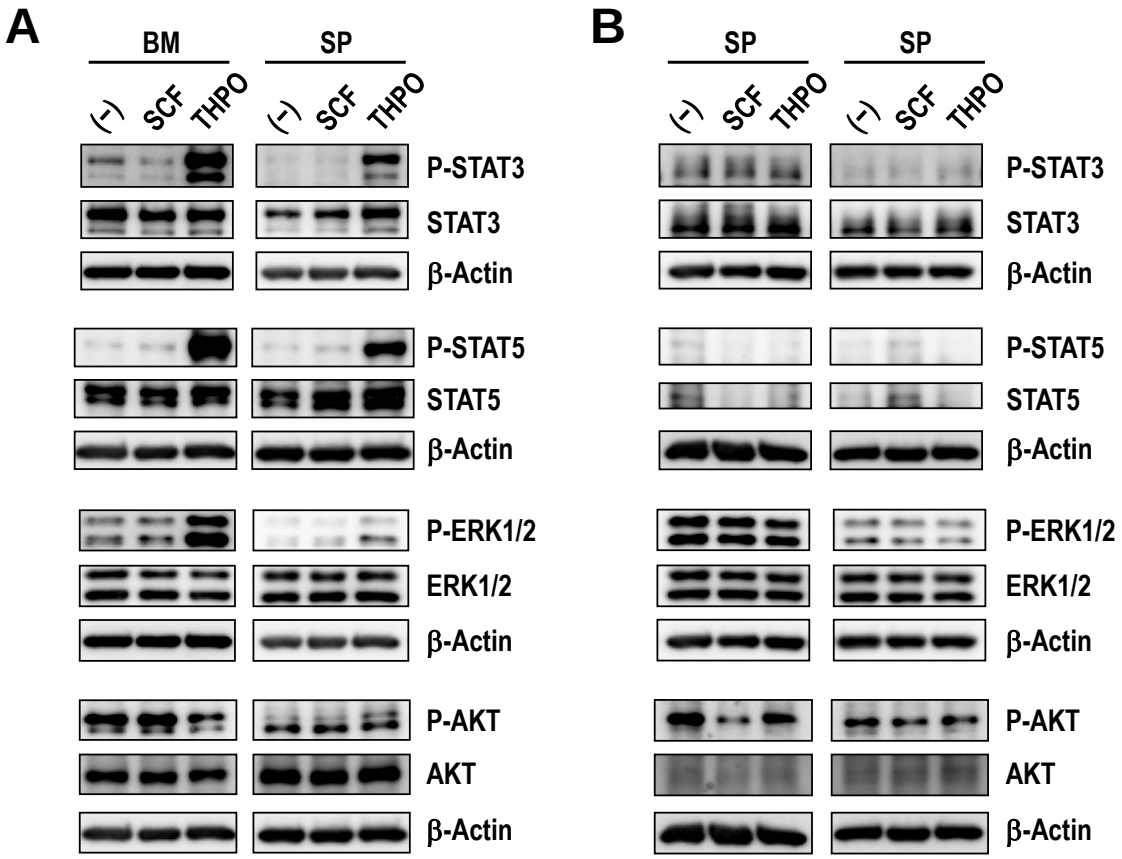

Figure 16. THPO induces phosphorylation of STAT3, STAT5, and ERK1/2 in Evi1 leukemia cells.

(A) BM- and SP-MNCs of Evi1 leukemia mice were serum-starved in α-MEM containing 1% BSA for 60 minutes and then stimulated with SCF or THPO in α-MEM containing 0.1% BSA for 60 minutes. Unstimulated cells were used as negative controls. The phosphorylation levels of STAT3, STAT5, ERK1/2, and AKT were analyzed by western blotting. (B) SP-MNCs were harvested from 2 independent MLL-ENL leukemia mice in which Mpl expression was not observed (shown in Figure 13). The phosphorylation levels of STAT3, STAT5, ERK1/2, and AKT were analyzed as described above.

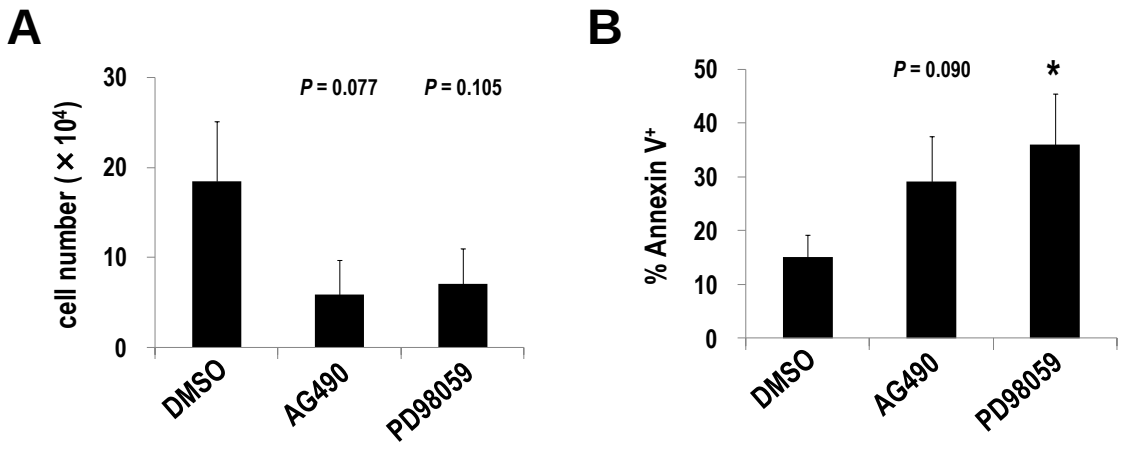

Figure 17. Pharmacologic inhibition of JAK/STAT and MEK/ERK pathways suppresses proliferation and induces apoptosis of CD41$^+$ Evi1 leukemia cells cultured on OP9 stromal cells.

CD41$^+$ cells were treated with dimethylsulfoxide (DMSO) as a vehicle control, a JAK2 inhibitor (AG490; 20 μM), or an MEK inhibitor (PD98059; 20 μM) on OP9 stromal cells in the presence of THPO for 7 days. (A) The number of viable cells was counted. Error bars indicate SD (n = 3; Dunnett's test). (B) The rate of apoptotic cells was determined by FACS. Error bars indicate SD (n = 4; *P < .05, Dunnett's test).

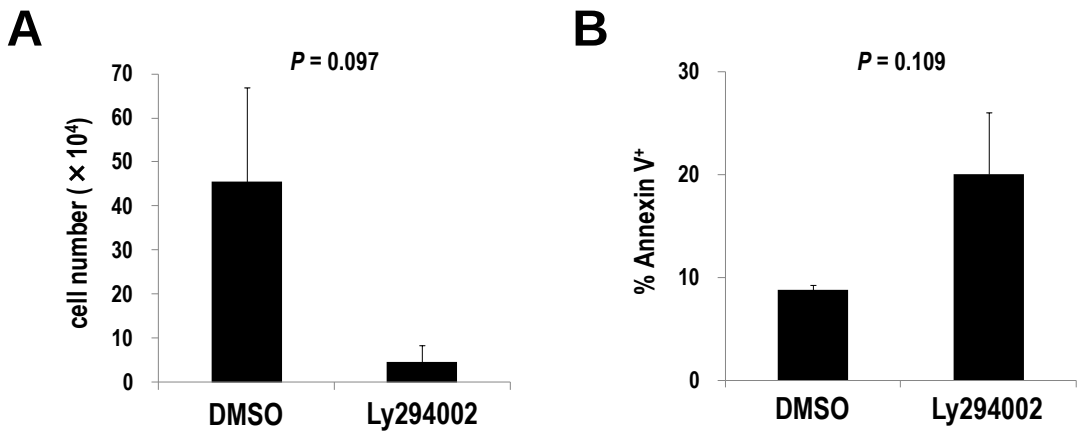

Figure 18. Pharmacologic inhibition of the PI3K/AKT pathway suppresses proliferation and induces apoptosis of CD41$^+$ Evi1 leukemia cells cultured on OP9 stromal cells.

CD41$^+$ cells were treated with DMSO as a vehicle control and a PI3K inhibitor (Ly294002; 5 μM) on OP9 stromal cells in the presence of THPO for 7 days. (A) The number of viable cells was counted. (B) The rate of apoptotic cells was determined by FACS. Error bars indicate SD in each graph (n = 3; Student *t* test).

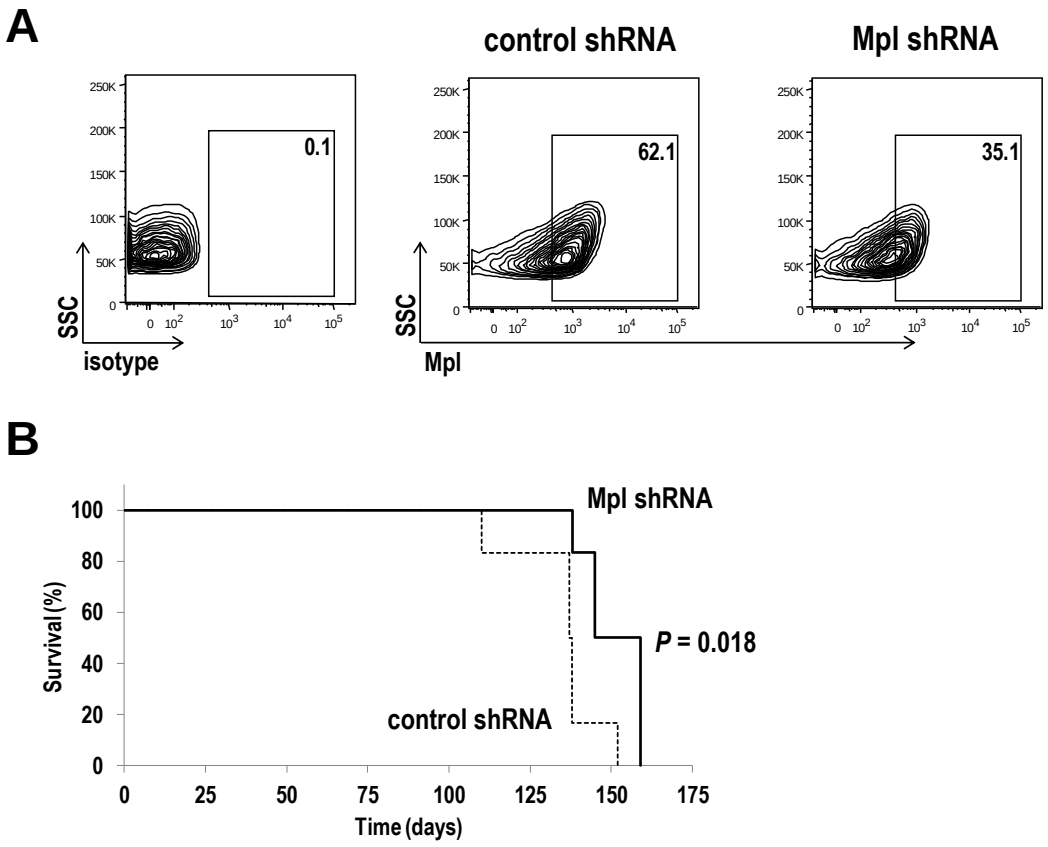

Figure 19. Knockdown of Mpl by shRNA transduction partially, but significantly, prolongs the survival of Evi1 leukemia mice.

(A) Evi1 leukemia BM cells were retrovirally transduced with Mpl shRNA or control shRNA. Transduced cells were then cultured on OP9 stromal cells in the presence of THPO. Cells were harvested and stained with an Alexa Fluor 647-labeled anti-mouse Mpl antibody. Evi1 leukemia cells expressing Mpl shRNA showed about 50% reduction of Mpl^+ cells compared with those expressing control shRNA. (B) Evi1 leukemia BM cells transduced with Mpl shRNA or control shRNA were transplanted into sublethally irradiated mice. The survival curves of mice transplanted with Mpl shRNA (n = 6; solid line) or control shRNA (n = 6; dotted line) are shown (P = .018, log-rank test).

BCL-xL upregulation via THPO/MPL signaling supports CD41$^+$ Evi1 leukemia cells

Because THPO/MPL signaling enhanced the anti-apoptotic property of CD41$^+$ Evi1 leukemia cells, I examined the expression patterns of several anti-apoptotic Bcl-2 family genes. Additionally, the finding that *BCL-2* was one of the candidate genes highly correlated with *EVI1* expression (Table 1) led me to explore the functional significance of Bcl-2 family genes in Evi1-related leukemogenesis. CD41$^+$ cells showed higher expression of *Bcl-xL* and *Bcl-2* than CD41$^-$ cells (Figure 20A). In contrast, *Mcl-1* expression levels were comparable between these fractions. Furthermore, BCL-xL was more highly expressed in CD41$^+$ cells at the protein level than in CD41$^-$ cells (Figure 20B). However, the expression of BCL-2 and MCL-1 was comparable in these fractions (Figure 20C–D). After serum starvation and subsequent stimulation with THPO, the expression of BCL-xL, but not BCL-2 and MCL-1, was upregulated in Evi1 leukemia cells (Figure 21). Thus, I assumed that BCL-xL is important for the growth and survival of Mpl$^+$ Evi1 leukemia cells. I examined whether WEHI-539, a highly specific BCL-xL inhibitor,[39] exerts an inhibitory effect on Evi1 leukemia cells cultured on OP9 feeder cells. WEHI-539 seemed to inhibit the growth and induce apoptosis of CD41$^+$ cells in a dose-dependent manner (Figure 22). On the contrary, the growth of CD41$^-$ cells was not affected by WEHI-539. These results indicate that THPO/MPL signaling supports the growth and survival of Evi1 leukemia cells via upregulating BCL-xL.

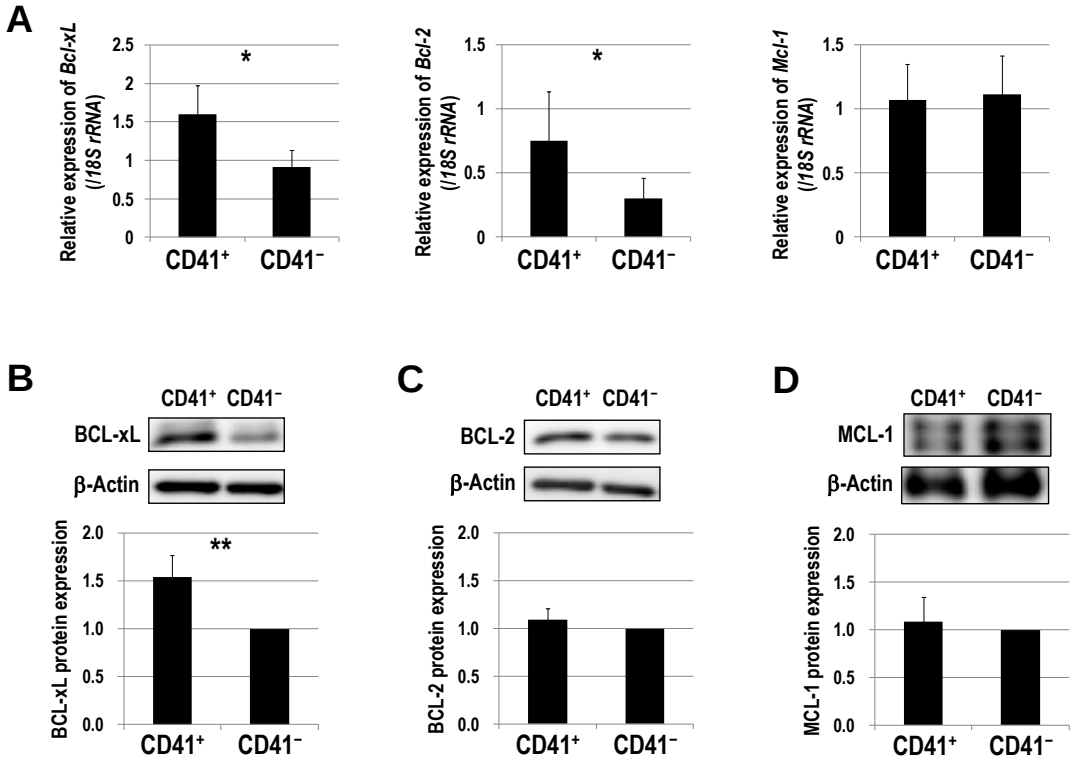

Figure 20. CD41$^+$ Evi1 leukemia cells show higher expression of BCL-xL than CD41$^-$ cells.

(A) Comparison of *Bcl-xL* (left), *Bcl-2* (middle), and *Mcl-1* (right) mRNA expression between CD41$^+$ and CD41$^-$ BM cells of Evi1 leukemia mice. CD41$^+$ and CD41$^-$ BM cells were sorted from 5 independent mice. Expression levels relative to normal c-kit$^+$ BM cells are presented. Error bars indicate SD (*P < .05, Student t test). (B–D) Comparison of protein expression of BCL-xL (B), BCL-2 (C), and MCL-1 (D) between CD41$^+$ and CD41$^-$ fractions by western blotting. Representative images and bar graphs showing quantified protein levels are presented. Expression levels were normalized to β-Actin expression as the internal control and represented as relative values to those of CD41$^-$ cells. Quantification was performed by ImageJ software. Error bars indicate SD (n = 5; **P < .01, Student t test).

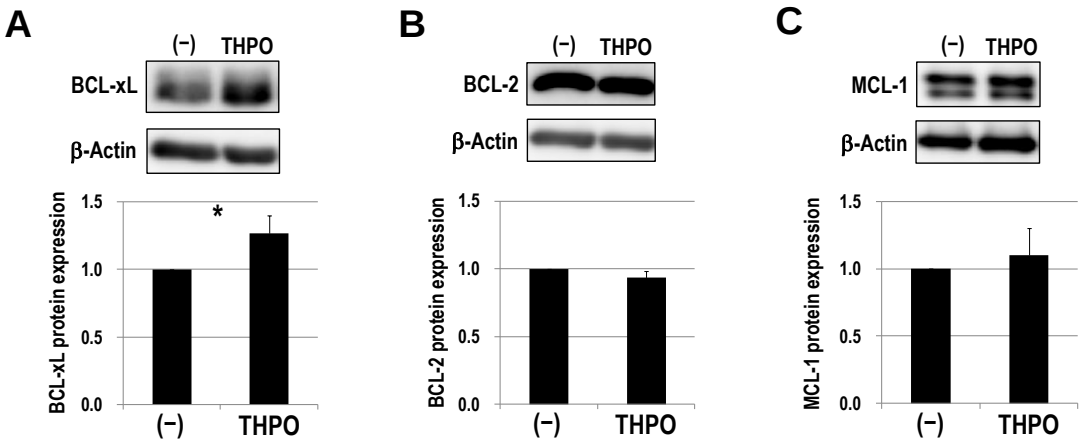

Figure 21. THPO upregulates BCL-xL expression in Evi1 leukemia cells.

Cryopreserved BM- or SP-MNCs from Evi1 leukemia mice were thawed and serum-starved in α-MEM containing 1% BSA for 3 hours, and then stimulated with or without THPO in α-MEM containing 0.1% BSA for 7 hours. Cells were washed with PBS and lysed for protein extraction. The expression levels of BCL-xL (A), BCL-2 (B), and MCL-1 (C) were determined by western blotting. Representative images and bar graphs showing quantified protein levels are presented. Quantification was performed as described in Figure 20. Error bars indicate SD (n = 4; **P* < .05, Student *t* test).

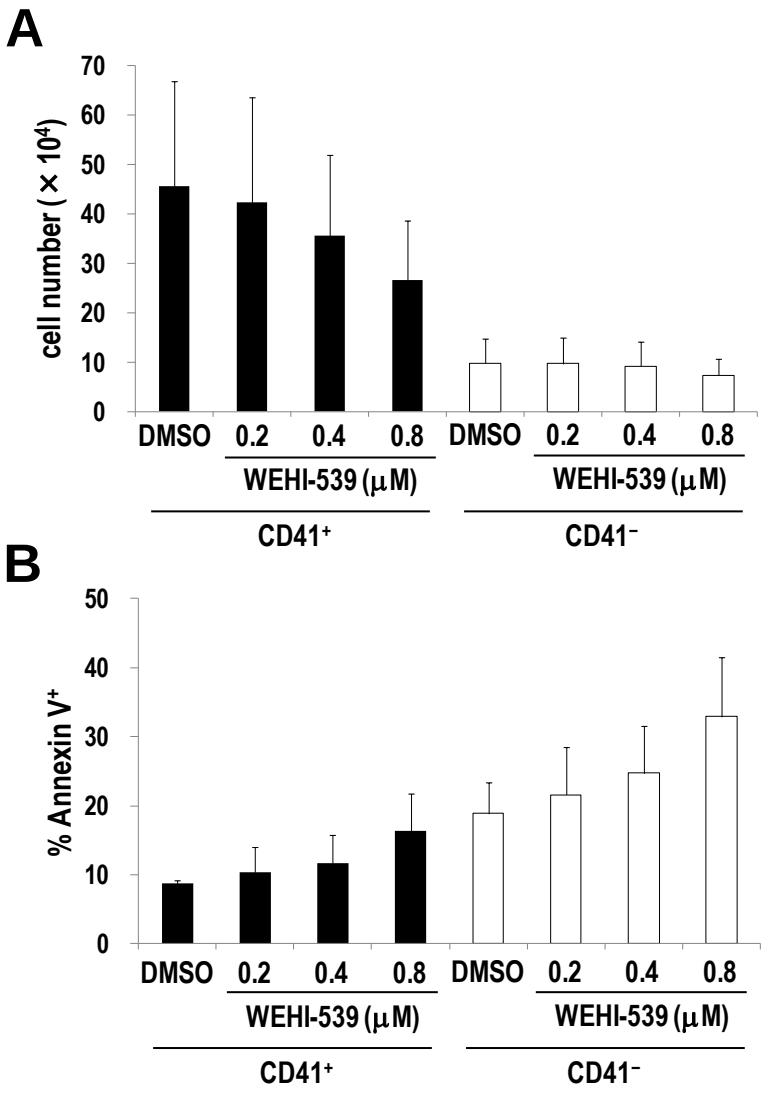

Figure 22. Pharmacologic inhibition of BCL-xL suppresses proliferation and induces apoptosis of CD41$^+$ Evi1 leukemia cells cultured on OP9 stromal cells.

CD41$^+$ or CD41$^-$ cells were treated with DMSO as a vehicle control or a BCL-xL inhibitor (WEHI-539; 0.2, 0.4, and 0.8 μM) on OP9 stromal cells in the presence of THPO for 7 days. (A) The number of viable cells was counted. Error bars indicate SD (n = 3). (B) The rate of apoptotic cells was determined by FACS. Error bars indicate SD (n = 3). Black and white bars represent the results from CD41$^+$ and CD41$^-$ cells, respectively. There was no significant difference between DMSO- and WEHI-539-treated groups (Dunnett's test).

CD41 is expressed in BM-MNCs derived from primary AML patients with *EVI1* expression

Several clinical studies reported that CD41 or CD61 expression is detected by FACS or immunohistochemistry in a subset of AML specimens with 3q abnormalities.[40-44] Therefore, I finally examined CD41 expression by FACS using 4 primary AML samples, one carrying a t(3;3) translocation and the others carrying an *MLL*-rearrangement (Table 4). Among them, $CD34^+$ cells derived from the t(3;3) patient and 1 *MLL*-rearranged patient more frequently expressed CD41 than those from the others (Figure 23A). Interestingly, $CD34^+$ cells of these 2 patients clearly expressed *EVI1* (Figure 23B–C). These results indicate that CD41 upregulation is also found in primary AML samples with *EVI1* expression, although further investigation using more clinical samples will be needed to confirm the relationship between *EVI1* and CD41.

Table 4. Clinical characteristics of the 4 patients with AML

Patient No.	Age	Sex	Disease status	Type	Cytogenetics	Blast (%)
1	33	F	Relapse 1	AML-MRC	46, XX, t(3;3)(q21;q26.2), der(11)add(11)(p11.2)add(11)(q21), inv(11)(p15q13)	51
2	68	F	Onset	AML (M5a)	46, XX, t(6;11)(q27;q23)	97
3	48	M	Induction failure	AML (M4)	46, XY, t(11;19)(q23;p13.1)	5
4	42	F	Induction failure	AML (M4)	46, XX, t(9;11)(p22;q23)	12.5

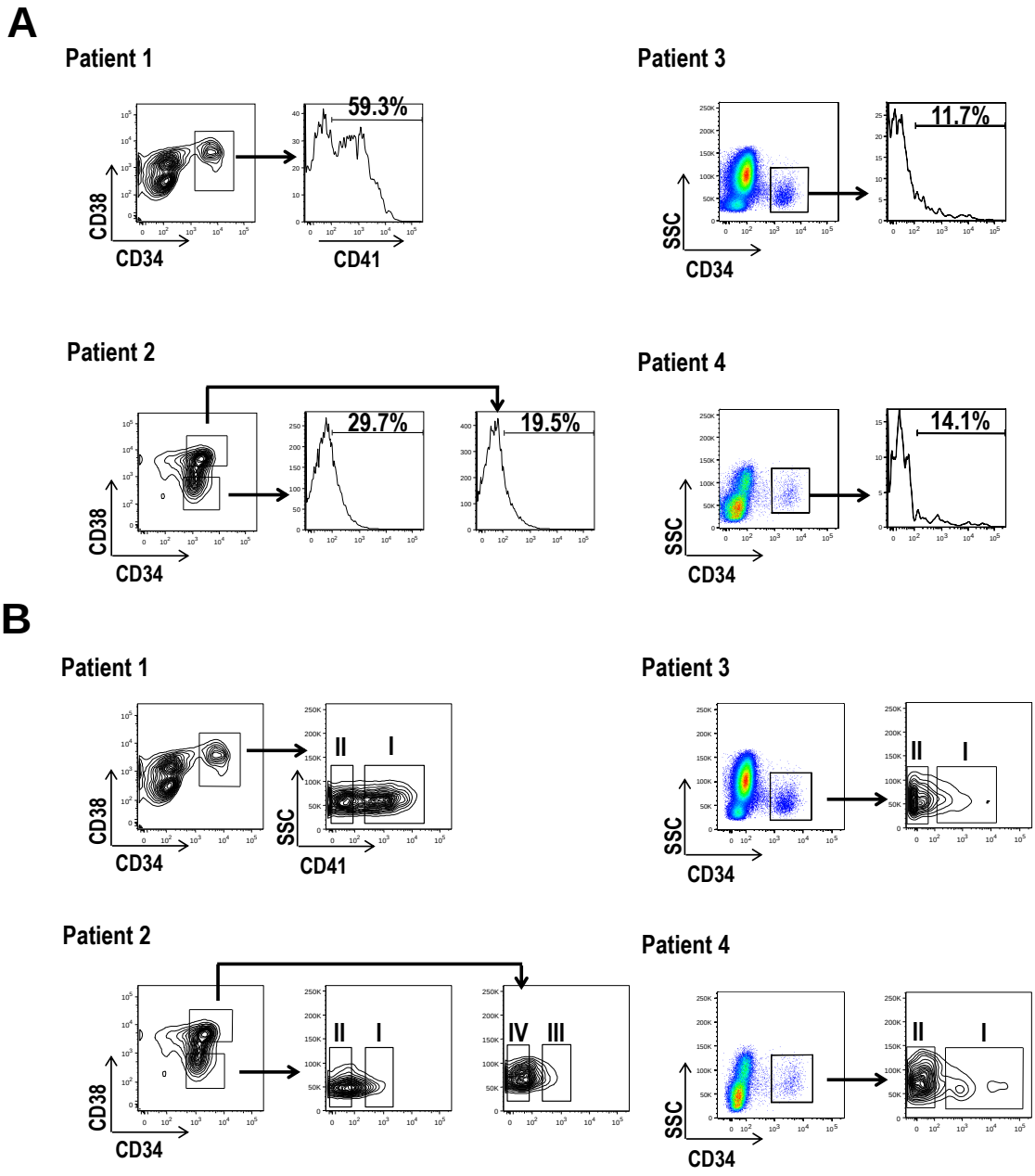

Figure 23. *EVI1* expression in CD34$^+$/CD41$^+$ cells derived from AML patients.
(A) BM-MNCs derived from 4 AML patients, one carrying a t(3;3) translocation (Patient 1) and the others carrying an *MLL*-rearrangement (Patient 2–4), were analyzed by FACS. Frequencies of CD41$^+$ cells within CD34$^+$, CD34$^+$/CD38$^-$, or CD34$^+$/CD38$^+$ fraction are presented. (B) For qPCR analysis, subfractions were sorted as follows: CD34$^+$/CD41$^+$ (I) and CD34$^+$/CD41$^-$ (II) for patient 1, 3, and 4; CD34$^+$/CD38$^-$/CD41$^+$ (I), CD34$^+$/CD38$^-$/CD41$^-$ (II), CD34$^+$/CD38$^+$/CD41$^+$ (III), and CD34$^+$/CD38$^+$/CD41$^-$ (IV) for patient 2.

C

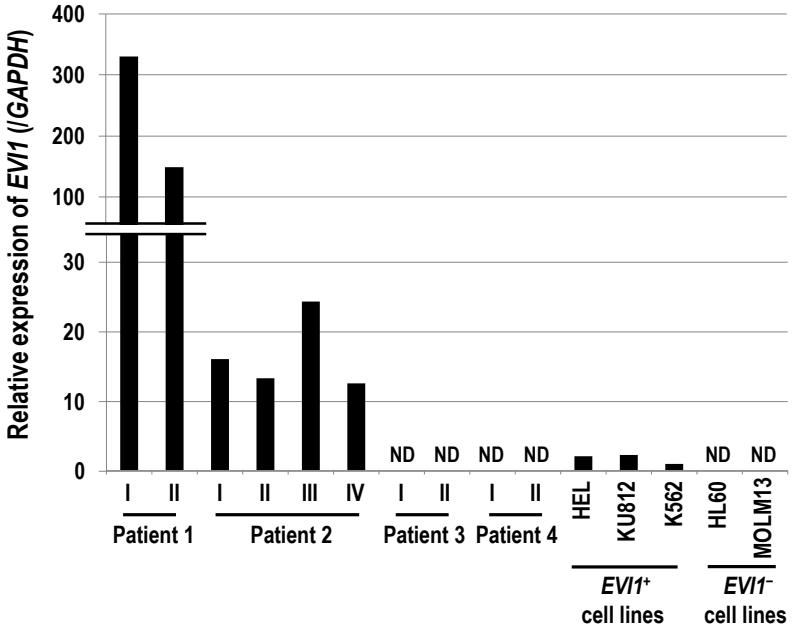

Figure 23. *EVI1* expression in CD34$^+$/CD41$^+$ cells derived from AML patients. (continued)

(C) *EVI1* expression was analyzed by qPCR in subfractions of primary AML cells shown in panel B, and *EVI1*$^+$ (HEL, KU812, and K562) and *EVI1*$^-$ (HL60 and MOLM13) cell lines. Expression levels relative to K562 cells are presented. ND means not detected. Clinical characteristics of the patients are presented in Table 4.

Discussion

In this study, I found that the expression of *ITGA2B* and *MPL* positively correlated with that of *EVI1* in AML patients and that a subfraction of BM and SP cells derived from Evi1 leukemia mice expressed both CD41 and Mpl. Several lines of evidence demonstrated that $CD41^+$ Evi1 leukemia cells not only contain immunophenotypically and functionally more immature cells but also exert a higher LIC in serial transplantation assays than $CD41^-$ cells. Moreover, the fact that THPO/MPL signaling supported the growth and survival of $CD41^+$ cells via upregulation of BCL-xL provides the novel molecular pathogenesis of Evi1 leukemia (Figure 24).

It has been shown that the THPO/MPL pathway is involved in leukemogenesis as well as megakaryopoiesis.[45] According to studies using primary AML samples, Mpl is expressed in 50% to 60% of AML cases,[46-49] and the majority of AML myeloblasts expressing Mpl proliferate in vitro in response to THPO.[46,47] In addition, inappropriately low levels of serum-circulating THPO, which recovered after effective chemotherapy, were reported in Mpl^+ AML patients, indicating that THPO is bound to Mpl^+ leukemia cells to promote their growth in vivo.[50] Recent reports that Mpl expression is upregulated in human AML cells harboring chromosomal translocation t(8;21)(q22;q22), which generates the *AML1-ETO* fusion gene, and THPO enhances their growth and self-renewing capacity further explain the biological relevance of this pathway in leukemogenesis.[51,52]

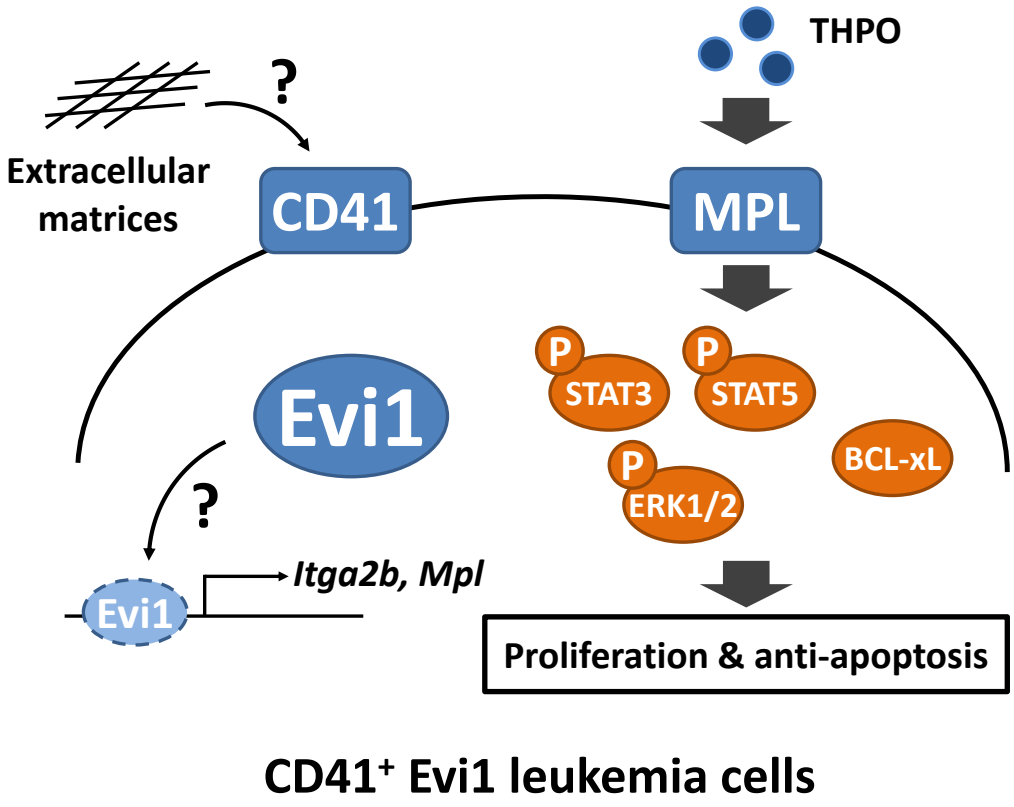

Figure 24. THPO/MPL signaling enhances growth and survival capacity of CD41$^+$ Evi1 leukemia cells.

Evi1 transduction in immature murine hematopoietic cells gives rise to CD41$^+$/Mpl$^+$ leukemia cells with a high LIC in vivo. THPO stimulation leads to phosphorylation of downstream pathways such as JAK/STAT and MEK/ERK, and upregulation of BCL-xL, which confers growth and survival capacity to CD41$^+$ Evi1 leukemia cells. It is still unclear whether Evi1 directly regulates *Itga2b* and *Mpl* expression and whether CD41 signaling is involved in leukemogenesis.

Here, I propose that THPO/MPL signaling is also implicated in the pathogenesis of Evi1-overexpressing AML that is clinically and molecularly distinct from AML1-ETO-positive AML, thus reinforcing the biological relevance of this pathway in leukemogenesis. Interestingly, there are some differences and similarities regarding the downstream cascades of the THPO/MPL pathway between Evi1 and AML1-ETO AML cells. In AML1-ETO leukemia models, the JAK/STAT and PI3K/AKT pathways rather than the MEK/ERK pathway are the important downstream cascades of THPO/MPL signaling.[51,52] In contrast, all 3 pathways were involved in the growth and survival of Evi1 leukemia cells, even though AKT activation was not induced by THPO (Figure 16A). Because Evi1 activates PI3K/AKT signaling by downregulating PTEN,[17] PTEN repression may have a predominant effect on AKT activation under the Evi1-overexpressed condition, compared with MPL-mediated activation of AKT. These findings indicate that the regulation of molecular networks downstream of MPL signaling varies in different cellular contexts. Here, I also demonstrated that BCL-xL expression was enhanced in $CD41^+$ Evi1 leukemia cells upon THPO stimulation and that pharmacologic inhibition of BCL-xL suppressed their growth and survival in vitro. Importantly, upregulation of BCL-xL through THPO/MPL signaling plays an essential role in sustaining the viability of normal megakaryocytes and leukemia cells carrying t(8;21)(q22;q22).[45,51,53] Therefore, I suppose that the THPO/MPL/BCL-xL cascade may serve as a common oncogenic driver for Mpl^+

AML cases irrespective of the cytogenetic or prognostic subclasses of AML. Although Table 1 implies the possible relevance of *BCL-2* with Evi1-related leukemogenesis, it is unclear whether BCL-2 is also important for the survival of Evi1 leukemia cells. Because BCL-2 protein expression was not induced by THPO stimulation (Figure 21B), other mechanisms might regulate BCL-2 expression in Evi1-overexpressing cells. On the other hand, *BCL-xL* gene was not found in Table 1. There are 2 possible reasons for this. One reason is that *BCL-xL* upregulation is not a specific feature of *EVI1*-high AML, because *BCL-xL* expression is positively correlated with a cluster of *EVI1*-negative AML such as AML with the chromosomal translocation t(8;21)(q22;q22) as described above. The other reason is that BCL-xL expression might relatively depend on post-translational regulation. A previous report demonstrating that THPO/MPL signaling prevents the cleavage of BCL-xL protein during normal megakaryopoiesis supports this speculation.[53] In contrast, Pradhan et al. recently reported that EVI1 directly induces *BCL-xL* expression through its binding to a *BCL-xL* promoter region in HT-29 colon carcinoma cells that express EVI1.[54] However, it is still unknown whether *BCL-xL* gene is a direct transcriptional target of EVI1 in human AML patients' cells.

While THPO/MPL signaling clearly enhanced the growth and survival of $CD41^+$ Evi1 leukemia cells, several experimental results presented in this study indicate that Evi1-related leukemogenesis may not completely depend on the THPO/MPL pathway.

Firstly, the THPO/MPL pathway seems to be dispensable for the growth of Evi1 leukemia cells in the semisolid culture system, because MethoCult M3434 medium does not contain THPO (Figure 8A). Moreover, addition of THPO to M3434 did not enhance the colony-forming activity of $CD41^+$ or $CD41^-$ cells (data not shown), raising the possibility that dependence on THPO/MPL signaling of Evi1 leukemia cells is reduced under semisolid culture conditions. The observation that Mpl expression on Evi1 leukemia cells was not maintained in M3434 culture (data not shown) may support this idea. Secondly, $CD41^-$ cells moderately possessed a LIC, because half of the mice transplanted with $CD41^-$ cells died from AML after a longer latency period than that in mice transplanted with $CD41^+$ cells (Figure 9). Furthermore, the limiting dilution transplantation assay revealed that in addition to $CD41^+$ fractions (Fr.1 and Fr.2), $CD41^-/CD150^+$ cells (Fr.3) also exhibited a high LIC (Figure 11B). Although Fr.3 might respond to THPO in vivo because Mpl expression in Fr.3 was significantly higher than that in $CD41^-/CD150^-$ cells (Fr.4) (data not shown), further experiments are required to uncover the molecular mechanism(s) that confer such a strong LIC to leukemia cells in Fr.3. For example, comprehensive gene expression analyses such as microarrays and high-throughput mRNA sequencing (RNA-Seq) could provide mechanistic insights into how each fraction exerts their leukemic properties.

Throughout the study, CD41 served as a surrogate marker for Mpl^+ Evi1 leukemia

cells. However, it is yet unclear whether CD41 signaling is responsible for the growth and survival of Evi1 leukemia cells. In megakaryocytes and platelets, CD41 and CD61 form a heterodimer and function as a receptor for several extracellular matrices such as fibronectin, vitronectin, and fibrinogen. For example, fibrinogen localized at vascular sinusoids in BM stimulates megakaryocytes through CD41/CD61 to induce proplatelet formation.[55] MWReg30, which was used here as an anti-mouse CD41 antibody, is known to block the function of CD41 on platelets and megakaryocytes.[55,56] Gekas and Graf[57] reported that MWReg30-treated murine HSCs show impaired long-term repopulation ability in vivo, suggesting that CD41/CD61 signaling is involved in the homing and lodging of normal HSCs in BM. However, I could not obtain clear evidence that CD41/CD61 is crucial for Evi1-mediated leukemogenesis, because $CD41^+$ cells stained with MWReg30 retained the capacity to induce secondary leukemia, and showed homing capacity to the BM and SP that was equivalent to that of $CD41^-$ cells (Figure 10). In addition, I found that the progression of AML was not delayed when Evi1 leukemia cells in which surface CD41 expression was partially interfered by an *Itga2b*-knockdown vector were transplanted into mice (data not shown). Thus, CD41/CD61 signaling might be dispensable for the proliferation or homing of Evi1 leukemia cells in vivo.

I found here that the expression of *ITGA2B* and *MPL* positively correlated with that of *EVI1* in AML patients and that overexpression of Evi1 in mouse BM cells gave rise

to $CD41^+$ and Mpl^+ leukemia cells. However, it is not clear how Evi1 induces the expression of megakaryocytic marker genes. One possibility is that Evi1 directly upregulates *Itga2b* and *Mpl* gene expression. However, there are no reports so far suggesting that these genes are the direct transcriptional targets of Evi1. Two groups have recently published the chromatin immunoprecipitation sequencing (ChIP-Seq) data of human ovarian carcinoma cell lines transduced with human *EVI1*[58] and that of Evi1-expressing murine leukemia cell lines.[59] In the human ovarian carcinoma cell dataset, 1 Evi1-bound peak was found in the *MPL* gene locus between exons 10 and 11. In the murine leukemia cell dataset, 1 Evi1-bound peak and 2 Evi1-bound peaks were found in estimated promoter regions of *Mpl* and *Itga2b* gene, respectively. These results raise a possibility that Evi1 could directly bind to these loci to activate gene expression via unidentified transcriptional machineries. Interestingly, 6 Evi1-bound peaks and 1 Evi1-bound peak were detected in the *BCL-xL* (*BCL2L1*) gene locus in the human and murine datasets, respectively, thus speculating some relevance of Evi1 in *BCL-xL* gene regulation. Alternatively, Evi1 may regulate the expression of key transcription factor(s) or physically interact with various epigenetic modifiers to increase *ITGA2B* and *MPL* expression. Recently, the existence of a distinct HSC subset biased toward the generation of $CD41^+$ megakaryocyte progenitors, whose maintenance depends on THPO, was reported.[60] Accordingly, Evi1 transduction might deregulate the epigenetic status of

HSPCs to render them partly similar to such a platelet-biased HSC fraction, resulting in increased generation of $CD41^+/Mpl^+$ transformed cells.

With regard to Mpl induction, it is still controversial whether Evi1 upregulates or downregulates Mpl expression. In our AML mouse model, Mpl was clearly expressed in Evi1 leukemia cells at both the mRNA and protein levels (Figure 12). On the contrary, *Mpl* expression decreases in hematopoietic cells from another mouse model in which transduction of human *EVI1* gene causes myelodysplastic syndrome (MDS).[61] In this model, EVI1 physically interacts with Gata1 to suppress the transcription of *Mpl* and the erythropoietin receptor, *Epor*.[20,62] One of the major differences between these mouse models is the species of the *Evi1* gene used, that is, human *EVI1* and mouse *Evi1* were used for the induction of MDS and AML, respectively. Laricchia-Robbio et al. proved that the proximal zinc finger domain (especially the first and sixth zinc fingers) of human EVI1 is crucial for direct interaction with Gata1.[20] Although mouse Evi1 used in this study also possesses a putative proximal zinc-finger domain equivalent to that of human EVI1, it is as yet unclear whether mouse Evi1 can repress Gata1 function through protein-protein interactions. From the perspective of *Gata1* gene expression, *Gata1* expression was upregulated in Evi1 leukemia BM cells, compared with that in normal $c\text{-}kit^+$ BM cells (data not shown). Given the fact that the transcription of *Gata1* is positively regulated by Gata1 itself,[63] it is unlikely that Gata1 is counteracted by Evi1 in our mouse model.

However, I cannot exclude the possibility that expression of Mpl and Gata1 is controlled in a disease-stage-specific manner during the process of developing Evi1 leukemia. As shown in Figure 9, leukemic symptoms emerged after a relatively longer latency (over 150 days) in transplantation assays, suggesting that the disease phenotype at earlier time points after transplantation may be different from that observed in the later leukemic stage. Therefore, monitoring of Gata1 and Mpl expression along with disease progression will help elucidate how their expression is regulated in the context of Evi1-overexpression.

For further confirming the importance of THPO/MPL signaling in Evi1-related AML, experiments using a number of *EVI1*$^+$ AML patients' specimens are required. Although I show here that CD41$^+$ HSPC fractions were found in 2 *EVI1*$^+$ AML patients' BM cells by FACS, I did not investigate whether these cells co-expressed MPL or whether THPO stimulation enhanced their growth and survival capacity. Thus, in the future, a variety of *EVI1*$^+$ AML BM cells might enable examining the correlation among EVI1, CD41, MPL, and BCL-xL at both mRNA and protein levels and identification of whether THPO modulates the leukemogenic property of *EVI1*$^+$ AML cells in biological assays as performed in this study. In addition, the surface CD41 expression in a subset of *EVI1*$^+$ AML cells is quite interesting in terms of AML diagnosis. Acute megakaryoblastic leukemia is a rare subtype of acute myeloid leukemia and is recognized as subtype AML-M7, within the French-American-British classification. Because one of the

hallmarks of AML-M7 is marked expression of megakaryocytic markers such as CD41 and CD61, one might think that CD41$^+$/*EVI1*$^+$ AML cases as exemplified in this study are classified as AML-M7. However, these cases were not diagnosed as AML-M7 (Table 4), partly due to the absence of megakaryoblastic features in their morphology. Therefore, abnormal CD41 expression can be observed in AML cases other than AML-M7, which might include those with high *EVI1* expression.

Finally, I mention the future therapies for *EVI1*$^+$ AML. As described, deregulated expression of Evi1 drives multiple oncogenic pathways in hematopoietic cells, which may account for the extremely poor therapeutic responses to conventional chemotherapy. Molecular targeted therapy is one of the most promising strategies for eradicating *EVI1*$^+$ leukemia cells. A previous report has suggested that rapamycin, an mTOR inhibitor, significantly prolongs the survival of Evi1 leukemia mice.[17] Morishita's group has proven the efficacy of neutralizing antibodies targeting the cell-to-niche interactions. For example, a neutralizing antibody against ITGA6 reduces the cell adhesion ability of *EVI1*$^+$ AML cells and renders them vulnerable to anti-cancer drugs.[29] More recently, all-*trans* retinoic acid (ATRA) was reported to reduce the clonogenic capacity of *EVI1*$^+$ AML cells both in vitro and in vivo by inducing their differentiation.[64] Here, I show that targeting the THPO/MPL/BCL-xL cascade might have beneficial effects on suppressing the LIC of Evi1-expressing leukemia cells. Based on these findings, combination therapies targeting

the downstream pathways of oncogenic EVI1 could be developed for treating *EVI1*$^{+}$ AML patients. Another possible therapy is to target EVI1 itself. Because EVI1 overexpression activates various undesirable oncogenic programs to form highly refractory AML, it might become a reasonable therapy to reduce EVI1 expression to normal or undetectable levels. One example is the report that a specific microRNA, miR-133, that can bind to the 3′ untranslated region of *EVI1* antagonizes *EVI1* expression to induce chemo-sensitivity in *EVI1*$^{+}$ AML cell lines.[65] The machinery for EVI1 transactivation might also become an ideal therapeutic target. Two recent reports have proven that juxtaposition of a distal GATA2 enhancer with the *EVI1* gene locus that is caused by 3q chromosomal rearrangements, leads to deregulated EVI1 expression.[66,67] Importantly, genomic excision of the enhancer or treatment with a BET-bromodomain inhibitor results in *EVI1* reduction, leading to growth inhibition and differentiation of *EVI1*$^{+}$ AML cell lines. Thus, these pioneering studies provide a rationale for antagonizing *EVI1* expression in EVI1-related AML treatment in the future.

In conclusion, I revealed in this study that THPO/MPL signaling enhances the growth and survival of CD41^{+} cells in a mouse model of Evi1 leukemia. These findings suggest the novel molecular mechanism of Evi1 leukemia through which Evi1 leukemia cells expressing Mpl may acquire growth and survival capacity by employing THPO as a cell-extrinsic factor. Accumulating discoveries regarding Evi1 functions have suggested

that the global epigenetic perturbations caused by Evi1 and the recently identified Evi1-related interactome[68] can drive multiple oncogenic molecular pathways, finally leading to AML development and maintenance. Although further investigations are needed to clarify how the expression of Mpl and other several megakaryocyte/platelet-related genes is regulated in the context of Evi1-overexpression, the present study provides insights into the pleiotropic roles of Evi1 in leukemogenesis.

Acknowledgments

I would like to express my sincere gratitude to Professor Mineo Kurokawa for his patient guidance and continuous encouragement throughout this study. I would like to offer special thanks to Dr. Shunya Arai for his helpful advice, suggestions, and technical guidance. I also would like to express my deepest gratitude to Dr. Naoko Watanabe-Okochi for providing me with valuable experimental tools and her kind cooperation.

I would like to extend my sincere gratitude to Dr. Yosuke Masamoto, Dr. Yuki Kagoya, and Dr. Takashi Toya for their helpful supports and valuable comments. I am also profoundly grateful to Ms. Yoshi Shimamura, Ms. Fumi Kaminaga, Ms. Mariko Yamamoto, Ms. Mayumi Kobayashi, the late Ms. Yuko Sawamoto, and all members of Professor Kurokawa's Laboratory for their excellent technical supports and valuable comments.

I would like to thank Dr. Hiroshi Miyazaki and many researchers of Kyowa Hakko Kirin Co., Ltd. for their constant encouragement.

Finally, I would like to thank my wife for her understanding, sincere encouragement, and continuing supports throughout my study.

References

1. Marcucci G, Haferlach T, Döhner H. Molecular genetics of adult acute myeloid leukemia: prognostic and therapeutic implications. *J Clin Oncol*. 2011;29(5):475-486.

2. Barjesteh van Waalwijk van Doorn-Khosrovani S, Erpelinck C, van Putten WL, Valk PJ, van der Poel-van de Luytgaarde S, Hack R, Slater R, Smit EM, Beverloo HB, Verhoef G, Verdonck LF, Ossenkoppele GJ, Sonneveld P, de Greef GE, Löwenberg B, Delwel R. High EVI1 expression predicts poor survival in acute myeloid leukemia: a study of 319 de novo AML patients. *Blood*. 2003;101(3):837-845.

3. Valk PJ, Verhaak RG, Beijen MA, Erpelinck CA, Barjesteh van Waalwijk van Doorn-Khosrovani S, Boer JM, Beverloo HB, Moorhouse MJ, van der Spek PJ, Löwenberg B, Delwel R. Prognostically useful gene-expression profiles in acute myeloid leukemia. *N Engl J Med*. 2004;350(16):1617-1628.

4. Lugthart S, van Drunen E, van Norden Y, van Hoven A, Erpelinck CA, Valk PJ, Beverloo HB, Löwenberg B, Delwel R. High EVI1 levels predict adverse outcome in acute myeloid leukemia: prevalence of EVI1 overexpression and chromosome 3q26 abnormalities underestimated. *Blood*. 2008;111(8):4329-4337.

5. Gröschel S, Lugthart S, Schlenk RF, Valk PJ, Eiwen K, Goudswaard C, van Putten WJ, Kayser S, Verdonck LF, Lübbert M, Ossenkoppele GJ, Germing U, Schmidt-Wolf I, Schlegelberger B, Krauter J, Ganser A, Döhner H, Löwenberg B, Döhner

K, Delwel R. High EVI1 expression predicts outcome in younger adult patients with acute myeloid leukemia and is associated with distinct cytogenetic abnormalities. *J Clin Oncol*. 2010;28(12):2101-2107.

6. Lugthart S, Gröschel S, Beverloo HB, Kayser S, Valk PJ, van Zelderen-Bhola SL, Jan Ossenkoppele G, Vellenga E, van den Berg-de Ruiter E, Schanz U, Verhoef G, Vandenberghe P, Ferrant A, Köhne CH, Pfreundschuh M, Horst HA, Koller E, von Lilienfeld-Toal M, Bentz M, Ganser A, Schlegelberger B, Jotterand M, Krauter J, Pabst T, Theobald M, Schlenk RF, Delwel R, Döhner K, Löwenberg B, Döhner H. Clinical, molecular, and prognostic significance of WHO type inv(3)(q21q26.2)/t(3;3)(q21;q26.2) and various other 3q abnormalities in acute myeloid leukemia. *J Clin Oncol*. 2010;28(24):3890-3898.

7. Swerdlow SH, Campo E, Harris NL, Jaffe ES, Pileri SA, Stein H, Thiele J, Vardiman JW. *WHO Classification of Tumours of Haematopoietic and Lymphoid Tissues*. 4th ed. Lyon, France: International Agency for Research on Cancer Press; 2008.

8. Kataoka K, Kurokawa M. Ecotropic viral integration site 1, stem cell self-renewal and leukemogenesis. *Cancer Sci*. 2012;103(8):1371-1377.

9. Balgobind BV, Lugthart S, Hollink IH, Arentsen-Peters ST, van Wering ER, de Graaf SS, Reinhardt D, Creutzig U, Kaspers GJ, de Bont ES, Stary J, Trka J, Zimmermann M, Beverloo HB, Pieters R, Delwel R, Zwaan CM, van den Heuvel-Eibrink MM. EVI1

overexpression in distinct subtypes of pediatric acute myeloid leukemia. *Leukemia*. 2010;24(5):942-949.

10. Matsuo H, Kajihara M, Tomizawa D, Watanabe T, Saito AM, Fujimoto J, Horibe K, Kodama K, Tokumasu M, Itoh H, Nakayama H, Kinoshita A, Taga T, Tawa A, Taki T, Shiba N, Ohki K, Hayashi Y, Yamashita Y, Shimada A, Tanaka S, Adachi S. EVI1 overexpression is a poor prognostic factor in pediatric patients with mixed lineage leukemia-AF9 rearranged acute myeloid leukemia. *Haematologica*. 2014;99(11):e225-227.

11. Jo A, Mitani S, Shiba N, Hayashi Y, Hara Y, Takahashi H, Tsukimoto I, Tawa A, Horibe K, Tomizawa D, Taga T, Adachi S, Yoshida T, Ichikawa H. High expression of EVI1 and MEL1 is a compelling poor prognostic marker of pediatric AML. *Leukemia*. 2015;29(5):1076-1083.

12. Yuasa H, Oike Y, Iwama A, Nishikata I, Sugiyama D, Perkins A, Mucenski ML, Suda T, Morishita K. Oncogenic transcription factor Evi1 regulates hematopoietic stem cell proliferation through GATA-2 expression. *EMBO J*. 2005;24(11):1976-1987.

13. Goyama S, Yamamoto G, Shimabe M, Sato T, Ichikawa M, Ogawa S, Chiba S, Kurokawa M. Evi-1 is a critical regulator for hematopoietic stem cells and transformed leukemic cells. *Cell Stem Cell*. 2008;3(2):207-220.

14. Kataoka K, Sato T, Yoshimi A, Goyama S, Tsuruta T, Kobayashi H, Shimabe M, Arai S, Nakagawa M, Imai Y, Kumano K, Kumagai K, Kubota N, Kadowaki T, Kurokawa

M. Evi1 is essential for hematopoietic stem cell self-renewal, and its expression marks hematopoietic cells with long-term multilineage repopulating activity. *J Exp Med*. 2011;208(12):2403-2416.

15. Sato T, Goyama S, Nitta E, Takeshita M, Yoshimi M, Nakagawa M, Kawazu M, Ichikawa M, Kurokawa M. Evi-1 promotes para-aortic splanchnopleural hematopoiesis through up-regulation of GATA-2 and repression of TGF-b signaling. *Cancer Sci*. 2008;99(7):1407-1413.

16. Shimabe M, Goyama S, Watanabe-Okochi N, Yoshimi A, Ichikawa M, Imai Y, Kurokawa M. Pbx1 is a downstream target of Evi-1 in hematopoietic stem/progenitors and leukemic cells. *Oncogene*. 2009;28(49):4364-4374.

17. Yoshimi A, Goyama S, Watanabe-Okochi N, Yoshiki Y, Nannya Y, Nitta E, Arai S, Sato T, Shimabe M, Nakagawa M, Imai Y, Kitamura T, Kurokawa M. Evi1 represses PTEN expression and activates PI3K/AKT/mTOR via interactions with polycomb proteins. *Blood*. 2011;117(13):3617-3628.

18. Senyuk V, Sinha KK, Li D, Rinaldi CR, Yanamandra S, Nucifora G. Repression of RUNX1 activity by EVI1: a new role of EVI1 in leukemogenesis. *Cancer Res*. 2007;67(12):5658-5666.

19. Laricchia-Robbio L, Premanand K, Rinaldi CR, Nucifora G. EVI1 Impairs myelopoiesis by deregulation of PU.1 function. *Cancer Res*. 2009;69(4):1633-1642.

20. Laricchia-Robbio L, Fazzina R, Li D, Rinaldi CR, Sinha KK, Chakraborty S, Nucifora G. Point mutations in two EVI1 Zn fingers abolish EVI1-GATA1 interaction and allow erythroid differentiation of murine bone marrow cells. *Mol Cell Biol*. 2006;26(20):7658-7666.

21. Kurokawa M, Mitani K, Irie K, Matsuyama T, Takahashi T, Chiba S, Yazaki Y, Matsumoto K, Hirai H. The oncoprotein Evi-1 represses TGF-beta signalling by inhibiting Smad3. *Nature*. 1998;394(6688):92-96.

22. Kurokawa M, Mitani K, Yamagata T, Takahashi T, Izutsu K, Ogawa S, Moriguchi T, Nishida E, Yazaki Y, Hirai H. The evi-1 oncoprotein inhibits c-Jun N-terminal kinase and prevents stress-induced cell death. *EMBO J*. 2000;19(12):2958-2968.

23. Izutsu K, Kurokawa M, Imai Y, Maki K, Mitani K, Hirai H. The corepressor CtBP interacts with Evi-1 to repress transforming growth factor beta signaling. *Blood*. 2001;97(9):2815-2822.

24. Vinatzer U, Taplick J, Seiser C, Fonatsch C, Wieser R. The leukaemia-associated transcription factors EVI-1 and MDS1/EVI1 repress transcription and interact with histone deacetylase. *Br J Haematol*. 2001;114(3):566-573.

25. Goyama S, Nitta E, Yoshino T, Kako S, Watanabe-Okochi N, Shimabe M, Imai Y, Takahashi K, Kurokawa M. EVI-1 interacts with histone methyltransferases SUV39H1

and G9a for transcriptional repression and bone marrow immortalization. *Leukemia*. 2010;24(1):81-88.

26. Senyuk V, Premanand K, Xu P, Qian Z, Nucifora G. The oncoprotein EVI1 and the DNA methyltransferase Dnmt3 co-operate in binding and de novo methylation of target DNA. *PLoS One*. 2011;6(6):e20793.

27. Chakraborty S, Senyuk V, Sitailo S, Chi Y, Nucifora G. Interaction of EVI1 with cAMP-responsive element-binding protein-binding protein (CBP) and p300/CBP-associated factor (P/CAF) results in reversible acetylation of EVI1 and in co-localization in nuclear speckles. *J Biol Chem*. 2001;276(48):44936-44943.

28. Saito Y, Nakahata S, Yamakawa N, Kaneda K, Ichihara E, Suekane A, Morishita K. CD52 as a molecular target for immunotherapy to treat acute myeloid leukemia with high EVI1 expression. *Leukemia*. 2011;25(6):921-931.

29. Yamakawa N, Kaneda K, Saito Y, Ichihara E, Morishita K. The increased expression of integrin alpha6 (ITGA6) enhances drug resistance in EVI1(high) leukemia. *PLoS One*. 2012;7(1):e30706.

30. Saito Y, Kaneda K, Suekane A, Ichihara E, Nakahata S, Yamakawa N, Nagai K, Mizuno N, Kogawa K, Miura I, Itoh H, Morishita K. Maintenance of the hematopoietic stem cell pool in bone marrow niches by EVI1-regulated GPR56. *Leukemia*. 2013;27(8):1637-1649.

31. Watanabe-Okochi N, Yoshimi A, Sato T, Ikeda T, Kumano K, Taoka K, Satoh Y, Shinohara A, Tsuruta T, Masuda A, Yokota H, Yatomi Y, Takahashi K, Kitaura J, Kitamura T, Kurokawa M. The shortest isoform of C/EBPβ, liver inhibitory protein (LIP), collaborates with Evi1 to induce AML in a mouse BMT model. *Blood*. 2013;121(20):4142-4155.

32. Arai S, Yoshimi A, Shimabe M, Ichikawa M, Nakagawa M, Imai Y, Goyama S, Kurokawa M. Evi-1 is a transcriptional target of mixed-lineage leukemia oncoproteins in hematopoietic stem cells. *Blood*. 2011;117(23):6304-6314.

33. Kagoya Y, Yoshimi A, Kataoka K, Nakagawa M, Kumano K, Arai S, Kobayashi H, Saito T, Iwakura Y, Kurokawa M. Positive feedback between NF-κB and TNF-α promotes leukemia-initiating cell capacity. *J Clin Invest*. 2014;124(2):528-542.

34. Kitamura T, Koshino Y, Shibata F, Oki T, Nakajima H, Nosaka T, Kumagai H. Retrovirus-mediated gene transfer and expression cloning: powerful tools in functional genomics. *Exp Hematol*. 2003;31(11):1007-1014.

35. Verhaak RG, Wouters BJ, Erpelinck CA, Abbas S, Beverloo HB, Lugthart S, Löwenberg B, Delwel R, Valk PJ. Prediction of molecular subtypes in acute myeloid leukemia based on gene expression profiling. *Haematologica*. 2009;94(1):131-134.

36. Li Z, Herold T, He C, Valk PJ, Chen P, Jurinovic V, Mansmann U, Radmacher MD, Maharry KS, Sun M, Yang X, Huang H, Jiang X, Sauerland MC, Büchner T,

Hiddemann W, Elkahloun A, Neilly MB, Zhang Y, Larson RA, Le Beau MM, Caligiuri MA, Döhner K, Bullinger L, Liu PP, Delwel R, Marcucci G, Lowenberg B, Bloomfield CD, Rowley JD, Bohlander SK, Chen J. Identification of a 24-gene prognostic signature that improves the European LeukemiaNet risk classification of acute myeloid leukemia: an international collaborative study. *J Clin Oncol*. 2013;31(9):1172-1181.

37. Qian H, Buza-Vidas N, Hyland CD, Jensen CT, Antonchuk J, Månsson R, Thoren LA, Ekblom M, Alexander WS, Jacobsen SE. Critical role of thrombopoietin in maintaining adult quiescent hematopoietic stem cells. *Cell Stem Cell*. 2007;1(6):671-684.

38. Yoshihara H, Arai F, Hosokawa K, Hagiwara T, Takubo K, Nakamura Y, Gomei Y, Iwasaki H, Matsuoka S, Miyamoto K, Miyazaki H, Takahashi T, Suda T. Thrombopoietin/MPL signaling regulates hematopoietic stem cell quiescence and interaction with the osteoblastic niche. *Cell Stem Cell*. 2007;1(6):685-697.

39. Lessene G, Czabotar PE, Sleebs BE, Zobel K, Lowes KN, Adams JM, Baell JB, Colman PM, Deshayes K, Fairbrother WJ, Flygare JA, Gibbons P, Kersten WJ, Kulasegaram S, Moss RM, Parisot JP, Smith BJ, Street IP, Yang H, Huang DC, Watson KG. Structure-guided design of a selective BCL-X(L) inhibitor. *Nat Chem Biol*. 2013;9(6):390-397.

40. Ohyashiki JH, Ohyashiki K, Shimamoto T, Kawakubo K, Fujimura T, Nakazawa S, Toyama K. Ecotropic virus integration site-1 gene preferentially expressed in

post-myelodysplasia acute myeloid leukemia: possible association with GATA-1, GATA-2, and stem cell leukemia gene expression. *Blood*. 1995;85(12):3713-3718.

41. Shi G, Weh HJ, Duhrsen U, Zeller W, Hossfeld DK. Chromosomal abnormality inv(3)(q21q26) associated with multilineage hematopoietic progenitor cells in hematopoietic malignancies. *Cancer Genet Cytogenet*. 1997;96(1):58-63.

42. Medeiros BC, Kohrt HE, Arber DA, Bangs CD, Cherry AM, Majeti R, Kogel KE, Azar CA, Patel S, Alizadeh AA. Immunophenotypic features of acute myeloid leukemia with inv(3)(q21q26.2)/t(3;3)(q21;q26.2). *Leuk Res*. 2010;34(5):594-597.

43. Yamamoto K, Okamura A, Sanada Y, Yakushijin K, Matsuoka H, Minami H. Marked thrombocytosis and dysmegakaryopoiesis in acute myeloid leukemia with t(2;3)(p22;q26.2) and EVI1 rearrangement. *Ann Hematol*. 2013;92(12):1713-1715.

44. Danilova OV, Levy NB, Kaur P. A case report of AML with myelodysplasia-related changes with aggressive course in association with t(3;8)(q26;q24). *J Hematopathol*. 2013;6(4):245–251.

45. Chou FS, Mulloy JC. The thrombopoietin/MPL pathway in hematopoiesis and leukemogenesis. *J Cell Biochem*. 2011;112(6):1491-1498.

46. Matsumura I, Kanakura Y, Kato T, Ikeda H, Ishikawa J, Horikawa Y, Hashimoto K, Moriyama Y, Tsujimura T, Nishiura T. Growth response of acute myeloblastic leukemia cells to recombinant human thrombopoietin. *Blood*. 1995;86(2):703-709.

47. Quentmeier H, Zaborski M, Graf G, Ludwig WD, Drexler HG. Expression of the receptor MPL and proliferative effects of its ligand thrombopoietin on human leukemia cells. *Leukemia*. 1996;10(2):297-310.

48. Wetzler M, Baer MR, Bernstein SH, Blumenson L, Stewart C, Barcos M, Mrózek K, Block AW, Herzig GP, Bloomfield CD. Expression of c-mpl mRNA, the receptor for thrombopoietin, in acute myeloid leukemia blasts identifies a group of patients with poor response to intensive chemotherapy. *J Clin Oncol*. 1997;15(6):2262-2268.

49. Takeshita A, Shinjo K, Izumi M, Ling P, Nakamura S, Naito K, Ohnishi K, Ohno R. Quantitative expression of thrombopoietin receptor on leukaemia cells from patients with acute myeloid leukaemia and acute lymphoblastic leukaemia. *Br J Haematol*. 1998;100(2):283-290.

50. Corazza F, Hermans C, D'Hondt S, Ferster A, Kentos A, Benoît Y, Sariban E. Circulating thrombopoietin as an in vivo growth factor for blast cells in acute myeloid leukemia. *Blood*. 2006;107(6):2525-2530.

51. Chou FS, Griesinger A, Wunderlich M, Lin S, Link KA, Shrestha M, Goyama S, Mizukawa B, Shen S, Marcucci G, Mulloy JC. The thrombopoietin/MPL/Bcl-xL pathway is essential for survival and self-renewal in human preleukemia induced by AML1-ETO. *Blood*. 2012;120(4):709-719.

52. Pulikkan JA, Madera D, Xue L, Bradley P, Landrette SF, Kuo YH, Abbas S, Zhu

LJ, Valk P, Castilla LH. Thrombopoietin/MPL participates in initiating and maintaining RUNX1-ETO acute myeloid leukemia via PI3K/AKT signaling. *Blood*. 2012;120(4):868-879.

53. Kozuma Y, Kojima H, Yuki S, Suzuki H, Nagasawa T. Continuous expression of Bcl-xL protein during megakaryopoiesis is post-translationally regulated by thrombopoietin-mediated Akt activation, which prevents the cleavage of Bcl-xL. *J Thromb Haemost*. 2007;5(6):1274-1282.

54. Pradhan AK, Mohapatra AD, Nayak KB, Chakraborty S. Acetylation of the proto-oncogene EVI1 abrogates Bcl-xL promoter binding and induces apoptosis. *PLoS One*. 2011;6(9):e25370.

55. Larson MK, Watson SP. Regulation of proplatelet formation and platelet release by integrin alpha IIb beta3. *Blood*. 2006;108(5):1509-1514.

56. Nieswandt B, Echtenacher B, Wachs FP, Schröder J, Gessner JE, Schmidt RE, Grau GE, Männel DN. Acute systemic reaction and lung alterations induced by an antiplatelet integrin gpIIb/IIIa antibody in mice. *Blood*. 1999;94(2):684-693.

57. Gekas C, Graf T. CD41 expression marks myeloid-biased adult hematopoietic stem cells and increases with age. *Blood*. 2013;121(22):4463-4472.

58. Bard-Chapeau EA, Jeyakani J, Kok CH, Muller J, Chua BQ, Gunaratne J, Batagov A, Jenjaroenpun P, Kuznetsov VA, Wei CL, D'Andrea RJ, Bourque G, Jenkins

NA, Copeland NG. Ecotopic viral integration site 1 (EVI1) regulates multiple cellular processes important for cancer and is a synergistic partner for FOS protein in invasive tumors. *Proc Natl Acad Sci U S A*. 2012;109(6):2168-2173.

59 Glass C, Wuertzer C, Cui X, Bi Y, Davuluri R, Xiao YY, Wilson M, Owens K, Zhang Y, Perkins A. Global Identification of EVI1 Target Genes in Acute Myeloid Leukemia. *PLoS One*. 2013;8(6):e67134.

60. Sanjuan-Pla A, Macaulay IC, Jensen CT, Woll PS, Luis TC, Mead A, Moore S, Carella C, Matsuoka S, Bouriez Jones T, Chowdhury O, Stenson L, Lutteropp M, Green JC, Facchini R, Boukarabila H, Grover A, Gambardella A, Thongjuea S, Carrelha J, Tarrant P, Atkinson D, Clark SA, Nerlov C, Jacobsen SE. Platelet-biased stem cells reside at the apex of the haematopoietic stem-cell hierarchy. *Nature*. 2013;502(7470):232-236.

61. Buonamici S, Li D, Chi Y, Zhao R, Wang X, Brace L, Ni H, Saunthararajah Y, Nucifora G. EVI1 induces myelodysplastic syndrome in mice. *J Clin Invest*. 2004;114(5):713-719.

62. Dickstein J, Senyuk V, Premanand K, Laricchia-Robbio L, Xu P, Cattaneo F, Fazzina R, Nucifora G. Methylation and silencing of miRNA-124 by EVI1 and self-renewal exhaustion of hematopoietic stem cells in murine myelodysplastic syndrome. *Proc Natl Acad Sci U S A*. 2010;107(21):9783-9788.

63. Tsai SF, Strauss E, Orkin SH. Functional analysis and in vivo footprinting

implicate the erythroid transcription factor GATA-1 as a positive regulator of its own promoter. *Genes Dev*. 1991;5(6):919-931.

64 Verhagen HJ, Smit MA, Rutten A, Denkers F, Poddighe PJ, Merle PA, Ossenkoppele GJ, Smit L. Primary acute myeloid leukemia cells with overexpression of EVI-1 are sensitive to all-trans retinoic acid. *Blood*. 2016;127(4):458-463.

65 Yamamoto H, Lu J, Oba S, Kawamata T, Yoshimi A, Kurosaki N, Yokoyama K, Matsushita H, Kurokawa M, Tojo A, Ando K, Morishita K, Katagiri K, Kotani A. miR-133 regulates Evi1 expression in AML cells as a potential therapeutic target. *Sci Rep*. 2016;6:19204.

66 Gröschel S, Sanders MA, Hoogenboezem R, de Wit E, Bouwman BA, Erpelinck C, van der Velden VH, Havermans M, Avellino R, van Lom K, Rombouts EJ, van Duin M, Döhner K, Beverloo HB, Bradner JE, Döhner H, Löwenberg B, Valk PJ, Bindels EM, de Laat W, Delwel R. A single oncogenic enhancer rearrangement causes concomitant EVI1 and GATA2 deregulation in leukemia. *Cell*. 2014;157(2):369-381.

67 Yamazaki H, Suzuki M, Otsuki A, Shimizu R, Bresnick EH, Engel JD, Yamamoto M. A remote GATA2 hematopoietic enhancer drives leukemogenesis in inv(3)(q21;q26) by activating EVI1 expression. *Cancer Cell*. 2014;25(4):415-427.

68. Bard-Chapeau EA, Gunaratne J, Kumar P, Chua BQ, Muller J, Bard FA, Blackstock W, Copeland NG, Jenkins NA. EVI1 oncoprotein interacts with a large and

complex network of proteins and integrates signals through protein phosphorylation. *Proc Natl Acad Sci U S A*. 2013;110(31):E2885-2894.